Taking advantage of luminescent lanthanide ions

Jean-Claude G. Bünzli*[a] and Claude Piguet*[b]

Received 7th June 2005
First published as an Advance Article on the web 20th September 2005
DOI: 10.1039/b406082m

Lanthanide ions possess fascinating optical properties and their discovery, first industrial uses and present high technological applications are largely governed by their interaction with light. Lighting devices (economical luminescent lamps, light emitting diodes), television and computer displays, optical fibres, optical amplifiers, lasers, as well as responsive luminescent stains for biomedical analysis, medical diagnosis, and cell imaging rely heavily on lanthanide ions. This *critical review* has been tailored for a broad audience of chemists, biochemists and materials scientists; the basics of lanthanide photophysics are highlighted together with the synthetic strategies used to insert these ions into mono- and polymetallic molecular edifices. Recent advances in NIR-emitting materials, including liquid crystals, and in the control of luminescent properties in polymetallic assemblies are also presented. (210 references.)

1. Lanthanides, light, and luminescence

Lanthanides, light, and luminescence are fascinating words, the former because it originates from the Greek word *lanthaneien* meaning "lying hidden" and the second because it is associated with life and with its big-bang origin. Presently, light is one of the most convenient vectors for conveying signals because it travels almost instantaneously and can easily reach regions of a complex molecular edifice that are not accessible to other molecular messengers. Light is easily detected by highly sensitive devices and techniques so that signalling methods based on the emission of light by a conveniently designed reporter are among the most sensitive ones known to date: single molecule detection is often within reach. Henceforth the interest of the biomedical community for light-emitting markers.

Luminescence has deep roots in mythology and the ancients were admiring, as well as afraid of, phenomena such as *aurora borealis*, the light of sea, luminous animals (fireflies, glow worms) or stones, lightning, phosphorescent wood, and the glow of the eyes. The discovery of the Bolognian stone by shoemaker Vincenzo Cascariolo in 1603, the first identified

[a]*École Polytechnique Fédérale de Lausanne (EPFL), Laboratory of Lanthanide Supramolecular Chemistry (LCSL), CH-1015, Lausanne, Switzerland. E-mail: jean-claude.bunzli@epfl.ch*
[b]*University of Geneva, Department of Inorganic, Analytical and Applied Chemistry, 30 Quai E. Ansermet, CH-1211, Geneva 4, Switzerland. E-mail: claude.piguet@chiam.unige.ch*

Jean-Claude Bünzli

Jean-Claude Bünzli is a physical-inorganic and analytical chemist by training and an active researcher in the field of co-ordination and supramolecular chemistry of the lanthanide ions. He earned a degree in chemical engineering in 1968 and a PhD in 1971 from the École Polytechnique Fédérale de Lausanne (EPFL). He spent two years at the University of British Columbia and one year at the Swiss Federal Institute of Technology in Zürich before being appointed at the University of Lausanne in 1974. Since 2001 he has been full professor of inorganic chemistry at EPFL. His research focuses mainly on the relationship between luminescent properties and structure of lanthanide-containing molecular edifices, on the use of lanthanide ions as luminescent probes and on the design of self-assembled building blocks for the synthesis of materials with predetermined photophysical and magnetic properties.

Claude Piguet

Claude Piguet studied chemistry at the University of Geneva where he received a PhD degree in 1989 in the field of biomimetic copper-dioxygen complexes. After postdoctoral periods in the groups of professors J.-M. Lehn, A. F. Williams, and J.-C. G. Bünzli, he initiated research projects in the field of lanthanide supramolecular chemistry. In 1995 he received the Werner Medal of the New Swiss Chemical Society and was appointed in 1999 as full professor of inorganic chemistry at the University of Geneva. His research interests include the design of discrete dlf multimetallic supramolecular edifices and the unravelling of the thermodynamic origin of their self-assembly processes, the programming of novel electronic functions depending on intermetallic communications, the molecular tuning of local dielectric constants, the preparation of lanthanide-containing metallomesogens and the development of paramagnetic NMR methods for addressing solution structures.

inorganic phosphor (actually barium sulfate doped by metal ions such as Zn^{II}, Sn^{II} and Cd^{II}), and of the element phosphor in 1669 are milestones in the long process which led to the understanding of the phenomena linked to light emission other than incandescence. In 1888, the German physicist Eilhardt Wiedemann coined the word "luminescence" for characterizing the light emission not conditioned by a rise in temperature.[1] In this review, we follow the IUPAC rules[2] regarding molecular luminescence spectroscopy in that we consistently use "fluorescence" for processes which occur without change in spin, typically $S_1 \rightarrow S_0$ or Yb($^2F_{5/2} \rightarrow {}^2F_{7/2}$) transitions, and "phosphorescence" for transitions implying a change in spin, typically $T_1 \rightarrow S_0$ or Eu($^5D_0 \rightarrow {}^7F_J$) transitions.

The lanthanides (Ce–Lu) are unique among the elements, barring the actinides, in resembling each other so markedly in their chemical properties, particularly oxidation states.[3,4] This is readily explained by the electronic configuration of the atoms and their derived ions, which essentially exist in their trivalent state Ln^{III} ([Xe]$4f^n$, n = 0–14) in aqueous solutions, in view of the various degrees of stabilization experienced by the 4f, 5d, and 6s orbitals upon ionization. The shielding of the 4f orbitals by the filled $5p^6 6s^2$ sub-shells results in special spectroscopic properties with parity-forbidden 4f–4f absorptions having very low molar absorption coefficients (typically $< 3\ M^{-1}\ s^{-1}$) and characteristic narrow-line emission, mostly in the visible and near infrared ranges. Luminescence has been instrumental in the discovery of several lanthanide elements (*cf.* the work of Crookes[5] and Urbain[6]). In turn, these elements have always played a prominent role in lighting and light conversion technologies (Auer mantles, incandescent lamps, lasers) and more recently in both cathode-ray[7] and plasma[8] displays.

Presently, attention focuses on several potential applications of luminescent lanthanide ions:[9] (i) their continuing use in the lighting industry for the engineering of lamp phosphors,[10] (ii) their ability to provide electroluminescent materials for organic light emitting diodes and optical fibres for telecommunications,[11] and (iii) their capacity to yield functional complexes for biological assays[12,13] and medical imaging purposes.[14]

1.1 Luminescent lanthanide ions

Most Ln^{III} ions are luminescent, but some are more emissive than others. The emissive properties of a lanthanide ion are governed by the facility with which its excited state(s) can be populated and the non-radiative de-activation paths minimized. To meet the first requirement, sensitization *via* the surroundings of the ion is often used (see next paragraph) so that the overall quantum yield of a lanthanide-containing molecular edifice is given by

$$Q_{Ln}^{L} = \eta_{sens}\, Q_{Ln}^{Ln} \qquad (1)$$

whereby Q_{Ln}^{L} and Q_{Ln}^{Ln} are the quantum yields resulting from indirect and direct excitation, respectively, while η_{sens} represents the efficacy with which electromagnetic energy is transferred from the surroundings onto the metal ion. The intrinsic quantum yield Q_{Ln}^{Ln} essentially depends on the energy gap between the lowest lying excited (emissive) state of the metal ion and the highest sublevel of its ground multiplet. The smaller this gap, the easier is its closing by non-radiative de-activation processes, for instance through vibrations of bound ligands, particularly high energy vibrations such as O–H. Fig. 1 displays partial energy diagrams for the lanthanide aquo ions,[15–20] while the main luminescent transitions are listed in Table 1. With respect to the energy gap requirement, it is obvious that Eu^{III}, Gd^{III}, and Tb^{III} are the best ions, with ΔE = 12 300 ($^5D_0 \rightarrow {}^7F_6$), 32 200 ($^6P_{7/2} \rightarrow {}^8S_{7/2}$) and 14 800 ($^5D_4 \rightarrow {}^7F_0$) cm^{-1}, respectively. However, Gd^{III} emits in the UV, and it is not very useful as luminescent probe for bioanalyses because its luminescence interferes with either emission or absorption processes in the organic part of the complex molecules. On the other hand, it can efficiently transfer energy onto Eu^{III} upon vacuum-UV excitation, resulting in the emission of two red photons (the so-called quantum cutting or down-conversion effect);[21] Gd^{III} is therefore a potential phosphor component for mercury-free fluorescent lamps. The sizeable energy gap displayed by Eu^{III} and Tb^{III} explains why luminescent probes containing these ions have been so popular during the last decades. Nevertheless, development of dual luminescent time-resolved immunoassays has also stirred interest for Sm^{III} (ΔE = 7 400, $^4G_{5/2} \rightarrow {}^6F_{11/2}$) or Dy^{III} (7 850 cm^{-1}, $^4F_{9/2} \rightarrow {}^6F_{3/2}$).[22,23] The other ions have all very low quantum yield in aqueous solutions and appear to be less useful with respect to similar applications. Pr^{III} emits both in visible and NIR ranges[24] and is often a component of solid state optical materials, in view of its ability of generating up-conversion, that is blue emission from $^3P_0$ upon two- or three-photon pumping of the $^1G_4$ or $^1D_2$ states.[25] Thulium is a blue emitter from its $^3P_0$, $^1D_2$, and $^1G_4$ levels and is used as such in electroluminescent devices;[11] it is the first Ln^{III} ion for which up-conversion has been demonstrated;[25] several other ions (Nd^{III}, Dy^{III}, Ho^{III}, Er^{III}) present up-conversion processes as well. In addition, Nd^{III}, Ho^{III}, Er^{III} and Yb^{III} have special interest in that they emit in the NIR spectral range and are very useful in the design of lasers (especially Nd^{III} with its line at 1.06 μm) and of telecommunication devices.[26] The telecommunication windows lie usually between 1 and 1.6 μm and Yb^{III} which emits slightly under 1 μm is less useful than Pr^{III} for instance (emitting at

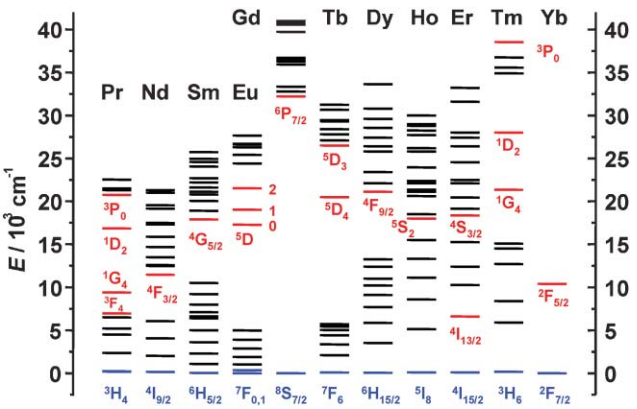

Fig. 1 Partial energy diagrams for the lanthanide aquo ions.[15,18,20] The main luminescent levels are drawn in red, while the fundamental level is indicated in blue.

Table 1 Main luminescent transitions of trivalent lanthanide aquo ions[15,18–20]

Ln	Excited state[a]	τ_{Rad}/ms[b]	End state[c]		Lumin. type[d]	λ/nm[e]	Emission color
Pr	$^1G_4$	n.a.	^3H_J	4–6	P	1300	NIR
	$^1D_2$	n.a.	^3F_J	2–4	P	890, 1060	NIR
	$^3P_0$	n.a.	^3H_J	4–6	F	525–680	Orange
Nd	$^4F_{3/2}$	0.42	^4I_J	9/2–15/2	F	1060	NIR
Sm	$^4G_{5/2}$	6.26	^6H_J	5/2–15/2	P	590	Orange
Eu	$^5D_0$	9.67	^7F_J	0–6	P	620	Red
Gd	$^6P_{7/2}$	10.9	$^8S_{7/2}$		P	312	UV
Tb	$^5D_4$	9.02	^7F_J	6–0	P	550	Green
Dy	$^4F_{9/2}$	1.85	^6H_J	15/2–5/2	P	570	Yellow-orange
Ho	$^5F_5$	n.a.	^5I_J	8–4	F	970, 1450	NIR
	$^5S_2$	0.37	^5I_J	8–4	F	540	Green
Er	$^4S_{3/2}$	0.66	^4I_J	15/2–9/2	F		
	$^4I_{13/2}$	n.a.	$^4I_{15/2}$		F	1530	NIR
Tm	$^1G_4$	n.a.	^3H_J	6–4	P		
Yb	$^2F_{5/2}$	1.2[f]	$^2F_{7/2}$		F	980	NIR

[a] Most luminescent excited states. [b] Radiative lifetime of the excited state for aquo ions, from ref. 17. Radiative lifetimes vary substantially from one compound to another. [c] Range of J-values indicated on the right hand side. [d] F: fluorescence; P: phosphorescence. [e] Approximate wavelength of most intense emission lines (or emission range). [f] For $[Yb(dtpa)]^{2-}$, from ref. 16.

1.33 μm) but it acts as an efficient sensitizer of Er^{III} (emitting at 1.55 μm).[26] Finally, the three ions Nd^{III}, Er^{III}, and Yb^{III} (as well as, partially, Pr^{III}) have recently gained in popularity because technical developments occurred which facilitate the detection of weak NIR emission and because efficient sensitizing groups have been explored. As a consequence of efficient light transmission of biological tissues in part of the NIR spectral range (0.9 to 1.5 μm approximately), lanthanide-containing luminescent probes based on these ions are now increasingly being used for time-resolved imaging of these tissues; cancer detection is obviously a highly sought for application.

Trivalent cerium (not shown on Fig. 1) emits a broad band spectrum in the range 370–410 nm due to the interconfigurational allowed 5d–4f transition and is not documented in this review, as is luminescence from the divalent and tetravalent ions (Ce^{IV}, Sm^{II}, Eu^{II}, Tb^{IV}, Yb^{II}, for instance).

1.2 Lighting up luminescent lanthanide ions

Most of the electronic transitions of the trivalent Ln^{III} ions involve a redistribution of electrons within the 4f sub-shell. Electric dipole selection rules forbid such transitions but these rules are relaxed by several mechanisms. An important one is the coupling with vibrational states, where a molecular vibration temporarily changes the geometric arrangement around the metal ion and, therefore, its symmetry. Other mechanisms which cause a breakdown of the selection rules are the *J*-mixing and the mixing with opposite-parity wavefunctions, such as 5d orbitals, ligand orbitals or charge transfer states. The coupling between these vibrational and electronic states and the 4f wavefunctions depends on the strength of the interaction between the 4f orbitals and the surrounding ligands; in view of the shielding of the 4f orbitals, the degree of mixing remains small, and so are the oscillator strengths of the f–f transitions. As a consequence, even if many lanthanide-containing compounds display a good quantum yield, direct excitation of the Ln^{III} ions rarely yields highly luminescent materials. Indirect excitation (called sensitization or antenna effect) has to be used and proceeds in three steps. First, light is absorbed by the immediate environment of the Ln^{III} ion through the attached organic ligands (chromophores). Energy is then transferred onto one or several excited states of the metal ion, and, finally, the metal ion emits light. A multitude of organic ligands bearing aromatic chromophores has been proposed for this purpose, derived, for instance, from bipyridine, terpyridine, triphenylene, quinoline, or substituted phenyl and naphthyl groups.

Although often discussed and modelled in terms of a simple ligand(S_1) → ligand(T_1) → Ln^* energy flow which can be optimized by adjusting the energy gap between the lowest ligand triplet state and the Ln^{III} emitting level,[27–29] sensitization of trivalent lanthanide ions is an exceedingly complex process involving numerous rate constants (Fig. 2).[30–32] Its fine-tuning requires the adjustment of several parameters and a comprehensive discussion is not given here, more detailed considerations being available in other review articles.[9,33,34] Both the singlet and triplet states of the ligand may transfer energy onto the metal ion and this transfer may be phonon-assisted; however, since the singlet state is short lived, this process is often not efficient. Classical considerations on the

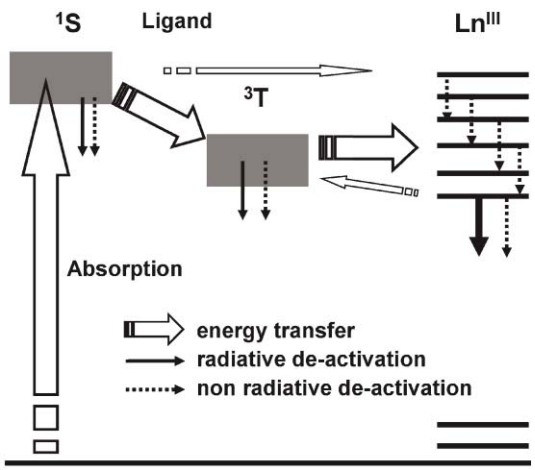

Fig. 2 Simplified diagram showing the main energy flow paths during sensitization of lanthanide luminescence *via* its surroundings (ligands).

ligand-to-metal energy transfer therefore take solely the energy of the triplet state into consideration. Or, rather, the energy of the lowest triplet state T_1 since elaborate ligands presently designed usually feature several triplet states. Within the frame of this simplified model, eqn (1) becomes:

$$Q_{Ln}^{L} = \eta_{isc}\, \eta_{et}\, Q_{Ln}^{Ln} \quad (2)$$

with η_{isc} representing the efficacy of the intersystem crossing process and η_{et} the effectiveness of the $^3\pi\pi^*$–Ln transfer. When excitation of T_1 leads to a relatively large expansion of the Ln–L distance, energy transfer occurs as long as the vibrational levels of T_1 are populated, that is the transfer stops when the lowest vibrational level is reached and T_1 phosphorescence takes over. On the other hand, if the Ln–L expansion is small, transfer is feasible as long as the triplet state is populated; if the rate constant of the transfer is large with respect to both radiative and non-radiative de-activation of T_1, the transfer becomes very efficient ($\eta_{sens} \approx 1$, eqn (1)). Two main mechanisms are usually invoked for the T_1-to-Ln^{III} transfer: (i) Dexter's (or exchange) mechanism, which involves a double electron transfer and requires a good overlap between the ligand and metal orbitals, and (ii) Förster's (or dipole–dipole) mechanism in which the dipole moment associated with the T_1 state couples with the dipole moment of the 4f orbitals and which is more likely for Ln^{III} ions. In addition, dipole–multipole transfers play non-negligible role in the sensitization of Ln^{III} ions.[30] If the main energy transfer path involves a dipole–dipole mechanism, its efficiency is given by:[31]

$$\eta_{et} = 1 - (\tau/\tau_0) = [1 + (R/R_0)^6]^{-1} \quad (3)$$

where τ and τ_0 are the lifetimes of the donor in presence and in absence of acceptor, respectively, R is the donor–acceptor distance and R_0 the distance for 50% transfer. It is specific for a given donor–acceptor pair, lies usually between 5 and 20 Å when a lanthanide ion is involved, and can be estimated from the spectroscopic data:

$$R_0^6 = 8.75 \times 10^{-25}\, \kappa^2\, Q_D\, n^{-4}\, J \quad (4)$$

with κ being an orientation factor (isotropic limit = 2/3), Q_D the quantum yield of the donor in absence of acceptor, n the refractive index and J the overlap integral between the emission spectrum of the donor and the absorption spectrum of the acceptor.

There are two other means for exciting the lanthanide ions. One takes advantage of the presence of charge-transfer states. This is essentially true for Sm^{III}, Eu^{III} and Yb^{III} and is often used when these ions are inserted into inorganic matrices, like in lamp phosphors.[35] Indeed, if such ligand-to-metal charge transfer states (LMCT) lie at high energy enough, they can transfer energy into the excited 4f-states; however, when their energy is close to the energy of the emitting level, they act as efficient quenchers of the 4f-luminescence.[36] In the case of Eu^{III}, excitation through LMCT is particularly efficient when E(LMCT) $\geqslant$ 40 000 cm^{-1} (see for instance Y_2O_3:Eu, with a quantum efficiency of 90%[37]); on the other hand Eu^{III} luminescence is almost completely quenched when E(LMCT) $< 25\,000\ cm^{-1}$.[32,36] The other excitation mode relies on energy transfer from a d-transition metal ion. For instance, Cr^{III} is a known activator of the Nd^{III} luminescence in YAG lasers[38] and, more recently, this excitation mode has stirred interest for the sensitization of NIR luminescence[39] and for increasing the apparent lifetimes of Nd^{III} and Yb^{III}.[40]

1.3 Preventing non-radiative de-activation processes

In addition to mastering the various processes leading to electronic excitation of the lanthanide ions, one has to prevent excited states from de-exciting *via* non-radiative processes. The overall de-activation rate constant (which is inversely proportional to the observed lifetime τ_{obs}) is given by:

$$k_{obs} = k^r + \sum_n k_n^{nr} = k^r + \sum_i k_i^{vibr}(T) + \sum_j k_j^{pet}(T) + \sum_k k_k'^{nr} \quad (5)$$

where k^r and k^{nr} are the radiative and non-radiative rate constants, respectively; the superscript 'vibr' points to vibrational processes while 'pet' refers to photo-induced electron transfer processes;[41] k' are rate constants associated with the remaining de-activation paths. De-activation through vibrations is especially effective and represents a major concern in the design of both inorganic and organic edifices. Multi-phonon processes are temperature dependent and the de-activation rate constant is also very sensitive to the metal–ligand distance since the interaction is of multipole–multipole nature, wherein the dipole–dipole component is predominant.[42] In aqueous solutions, interaction with water (both in the inner and outer coordination sphere of the Ln^{III} ion) leads to a severe quenching of the metal luminescence *via* O–H vibrations. Although detrimental to the design of highly luminescent edifices, this phenomenon can be used to assess the number of water molecules q interacting in the inner coordination sphere and several approximate phenomenological equations have been proposed, based on the assumptions that O–D oscillators do not contribute to de-activation and that all the other de-activation paths are the same in water and in deuterated water, and can henceforth be assessed by measuring the lifetime in the deuterated solvent:[43,44]

$$q = A\cdot(k_{H2O} - k_{D2O} - B) - C$$

where A, B, and C are phenomenological Ln-depending parameters determined using series of compounds with known hydration numbers. The corrective factor B has the same units as k and accounts for the presence of other de-activating vibrations (*e.g.* N–H or C–H oscillators). Such relationships, which exist for Nd, Sm, Eu, Tb, Yb are to be used with care and with the right calibration, given the hypotheses implied. They are nevertheless very useful and can be extended to other solvents, for instance alcohol.

The best way to minimize vibration-induced de-activation processes is to design a rigid metal-ion environment, free of high-energy vibrations and protecting the Ln^{III} ion from solvent interaction. Such an environment also contributes to reduce collision-induced de-activation in solution. Further protection may be gained by inserting the luminescent edifice

into micelles, a stratagem often used in bioanalyses. Finally, both photo-induced electron transfer from the ligand to the metal ion, resulting in a reduction of Ln^{III} into Ln^{II} (especially sensitive in the case of Eu^{II}) with a concomitant quenching of the metal-centred luminescence, and energy back transfer (see Fig. 2) have to be avoided by an adequate ligand design.

2. In search of efficient chelates

2.1 The chemical challenge

In addition to the features discussed above with respect to energy-transfer processes and minimization of non-radiative de-activation, the Ln^{III} environment in a lanthanide-containing luminescent probe must also fulfil several other requirements: high thermodynamic stability, kinetic inertness, and a saturated co-ordination sphere. Given the large lability of lanthanide ions and their need for high co-ordination numbers,[45] this poses a real challenge to synthetic chemists who have come up with several strategies to meet it, briefly described below. Furthermore, in case of bio-analyses, the luminescent probe has to comply with biochemical aspects as well, especially if the probe is to be used *in vivo*.

In aqueous solutions, the enthalpy and entropy changes upon complex formation between Ln^{III} cations and many ionic ligands is predominantly influenced by changes in hydration of both the cation and the ligand(s). Complexation results in a decrease in hydration, yielding a positive entropy change favourable to the complexation process. On the other hand, dehydration is endothermic and contribution from bond formation between the cation and the ligand(s) often does not compensate this unfavourable energy contribution to the variation in Gibbs free energy so that the overall complexation process is generally entropy driven. Therefore, it is advantageous to resort to polydentate ligands for building a co-ordination environment around Ln^{III} ions. During the last decades, inorganic chemists have come up with a number of imaginative strategies to insert Ln^{III} ions into functional edifices using such polydentate ligands.

A classical approach: linear polydentate and multifunctional ligands. Numerous ligands fall into this category, so that we shall only mention three large classes of ligands which have produced interesting Ln^{III} complexes. Polyaminocarboxylates have played a special role in Ln^{III} co-ordination chemistry since publication of the crystal structure of the La^{III} complex with edta definitively convinced the chemical community that Ln^{III} ions frequently possess co-ordination numbers larger than 6 (here 10). With log$K$ in the range 15–20, $[Ln(edta)]^-$ complexes are quite stable and consequently, the aminocarboxylate complexing unit has been grafted on numerous substrates, including macrocycles (*e.g.* in dota, 1,4,7,10-tetraaza-cyclododecane-*N*, *N′*, *N″*,*N‴*-tetraacetic acid, log$K$'s in the range 23–25).[46] Stability of these complexes arises from the combination of large entropic effects due to de-solvation of the aqua-ion and charge compensation occurring upon complexation, and the formation of strong ionic bonds with the carboxylate units, including the formation of stable five-membered chelate rings.[47]

Another efficient co-ordinating unit leading to five-membered chelate rings is β-diketonate. Rare earth β-diketonates were prepared as early as 1897 by G. Urbain and they are among the most investigated Ln^{III} co-ordination compounds, useful in a wealth of applications, ranging from complexation agents in solvent–solvent extraction processes, to NMR shift reagents, luminescent probes for time-resolved immunoassays, and electroluminescent materials. The bidentate nature of the chelating moiety, however, leads often to hexa-co-ordinated tris-complexes which complete their co-ordination sphere by adding two water molecules; detrimental to luminescent properties, these molecules can nevertheless be easily replaced by chromophores such as phenanthroline or bipyridine leading to highly luminescent ternary complexes.[48]

Acyclic Schiff base derivatives represent a resourceful class of compartmental ligands which are prepared by self-condensation of appropriate formyl and amine precursors. The condensation reaction is simple and generally leads to the desired product in high yield. Literature data on Ln^{III} mono- and bimetallic complexes, as well as on 4f–d transition metal bimetallic entities with these derivatives are abundant and have been reviewed recently.[49] Extension to multimetallic systems and to complexes with 5f elements is straightforward. Appropriate choice in the number and nature of the coordinating atoms assures a well defined co-ordination environment so that multimetallic systems with metal ions at pre-defined distances may be designed, which are most helpful in the study of magnetic interactions and energy transfer processes.

Macrocyclic receptors[50]. The idea behind the design of such ligands is to build a pre-organized cavity bearing several donor atoms generating suitable interactions with the metal ion (*i.e.* hard–hard or soft–soft in HSAB-theory terms) and with a cavity diameter well adapted to the size of the guest cation (lock-and-key principle). In this way, reorganization energy of the ligand upon complexation is minimized. Lanthanide macrocyclic chemistry started in the late 1960's when the need for NMR shift reagents induced the study of lanthanide phthalocyanines and porphyrins.[51] Two other classes of macrocyclic receptors were developed soon after as model ligands for the transport of cations through biological membranes, coronands (initially, crown ethers) and cryptands which were tested with variable success with the Ln^{III} ions.[52] Indeed, the difference in ionic radius between lanthanum and lutetium amounts to only 0.15 Å (for co-ordination number 9) while the ionic radius of two consecutive lanthanide ions differs by a mere 0.01–0.015 Å,[45] that is a fine tuning of the receptor to accommodate a specific Ln^{III} ion is out of reach, except possibly for the selective complexation of larger *versus* smaller ions, or *vice-versa*. This remark is also valid for lanthanide complexes with two series of macrocycles which were studied starting in the mid 1970's: simple calixarenes[53–55] and Schiff base derivatives.[49]

Therefore, another strategy was soon developed, based on the induced fit concept, which uses flexible receptors in order to optimize the interactions between the donor atoms and the metal ion. In fact, the co-ordination environment is built upon complexation thanks to the flexibility introduced into the complexation agent, which is now termed "predisposed

ligand''. These receptors are either large macrocycles able to wrap around the guest or small macrocycles fitted with pendant arms. The latter approach has proved to be very successful, particularly with calixarene[53] and cyclen (1,4,7,10-tetraazadodecane)[56] derivatives, which have been fruitfully used for the design of contrast agents for medical imaging,[57] receptors for radiopharmaceuticals[58] and luminescent sensors.[59]

Podands. The induced fit approach can also be conducted in an efficient way by designing podands. Here the functionalized pendant arms are no more attached onto a potentially co-ordinating macrocycle but simply on a single atom (boron, nitrogen, carbon, or transition metal ions) or a small aromatic ring such as benzene or triazine. This strategy is particularly useful when the design of a lanthanide-containing molecular edifice requires bidentate or tridentate pendant arms. Their grafting onto macrocycles is indeed not always straightforward from a synthetic standpoint. Ligands with four arms are usually built from small aromatic rings, while tri-armed receptors are often engineered from a single atom. The number of donor atoms can be easily varied by changing both the number of arms and their denticity. However, these ligands are less predisposed than the macrocycles fitted with pendant arms and the orientation of the arms to put the hosting cavity together requires more conformational work, which is detrimental to the stability of the final molecular edifice. One remedy is to profit from non-covalent interactions, such as H-bonding[60] or π-stacking interactions, or to start from a transition-metal podate[61] to position the arms in the right conformation prior to complexation.

Self-assembly processes. In going from pre-organized to predisposed receptors, one benefits from simplified synthetic procedures. The next step is to resort to metallosupramolecular chemistry and take advantage of both the high electric field generated by the Ln^{III} ions and weak intermolecular interactions to self-assemble small co-ordinating units around a metal ion. Application to co-ordination chemistry is relatively recent[62] and has immediately produced fascinating bi- and tri-dimensional functional edifices.[63] In our laboratories, we have produced large libraries of mono- and di-topic ligands which self assemble with Ln^{III} ions to yield monometallic and bimetallic 4f–4f and d–4f triple-helical edifices[64] with predetermined physico-chemical properties. Theoretical and rational modelling of the self-assembly of these helicates in now at hand, which enable a more rational approach[65] and extension to multimetallic systems,[66] so that self-assembly processes slowly emerge as a privileged strategy for the engineering of elaborate multimetallic edifices and devices.

2.2 Analytical sensors

In analytical sensors, the metal-centred luminescence is modulated by a process depending on the concentration of the analyte and involving reversible binding of the latter. Examination of Fig. 2 suggests that luminescence modulation can be induced through three main mechanisms (Fig. 3). Firstly, one may act directly onto the Ln^{III} ion. For instance, since luminescence intensity is highly sensitive to the presence

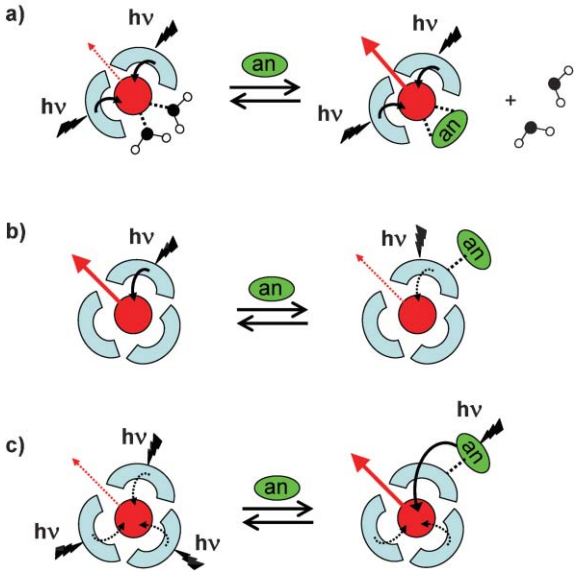

Fig. 3 Typical situations occurring in the modulation of lanthanide emission through reversible binding of an analyte (an): (a) direct influence on the Ln^{III} luminescence, (b) influence on the ligand photophysical properties, and (c) addition of a sensitizing analyte onto a poorly luminescent lanthanide-containing sensor (note that situations b and c could be reversed, *i.e.* sensitization *versus* quenching).

of water molecules in the inner co-ordination sphere, an unsaturated co-ordination environment provided by the ligand(s) will allow water binding. When these quenching water molecules are displaced, for instance by reversible binding of an anion, emission intensity is restored and the lifetime of the excited level lengthened. Secondly, one may influence the photophysical properties of the ligand, either of its singlet state or of its triplet state. For instance, inter- or intra-molecular quenching of the $^1\pi\pi^*$ state can be induced by electron or charge transfer processes involving the ligand and/or the Ln^{III} ion. Alternatively, a reversible binding process may influence the energy of the $^1\pi\pi^*$ state and, consequently, the efficiency of the isc transfer. The energy of the triplet state may also be altered by reversible binding, affecting the rate of energy transfer onto the metal ion (or of back transfer), henceforth the luminescence intensity. On the other hand, one may resort to direct quenching of the $^3\pi\pi^*$ state by, for instance, molecular oxygen. Thirdly, the analyte itself may be used as either sensitising moiety for the Ln^{III} luminescence or possibly as a quencher. Direct binding to the metal ion is not necessarily required, as demonstrated by a polyaromatic hydrocarbon (PAH) sensor based on an initially poorly luminescent Tb^{III} complex with a cyclodextrin–dtpa complexation unit. Efficient energy transfer from the PAH onto the metal ion is initiated through binding in the cyclodextrin cavity (Scheme 1).[67] Luminescent lanthanide sensors for pH, pO_2 and anions such as halides, hydrogencarbonate and hydrogenphosphate have been reviewed,[59,68] so that we only describe selected examples here.

Metal ion sensors. Several metal ion sensors have been proposed, mostly for the analysis of biologically relevant cations. The cyclen-based **Eu·L1** complex (Scheme 1) bearing a

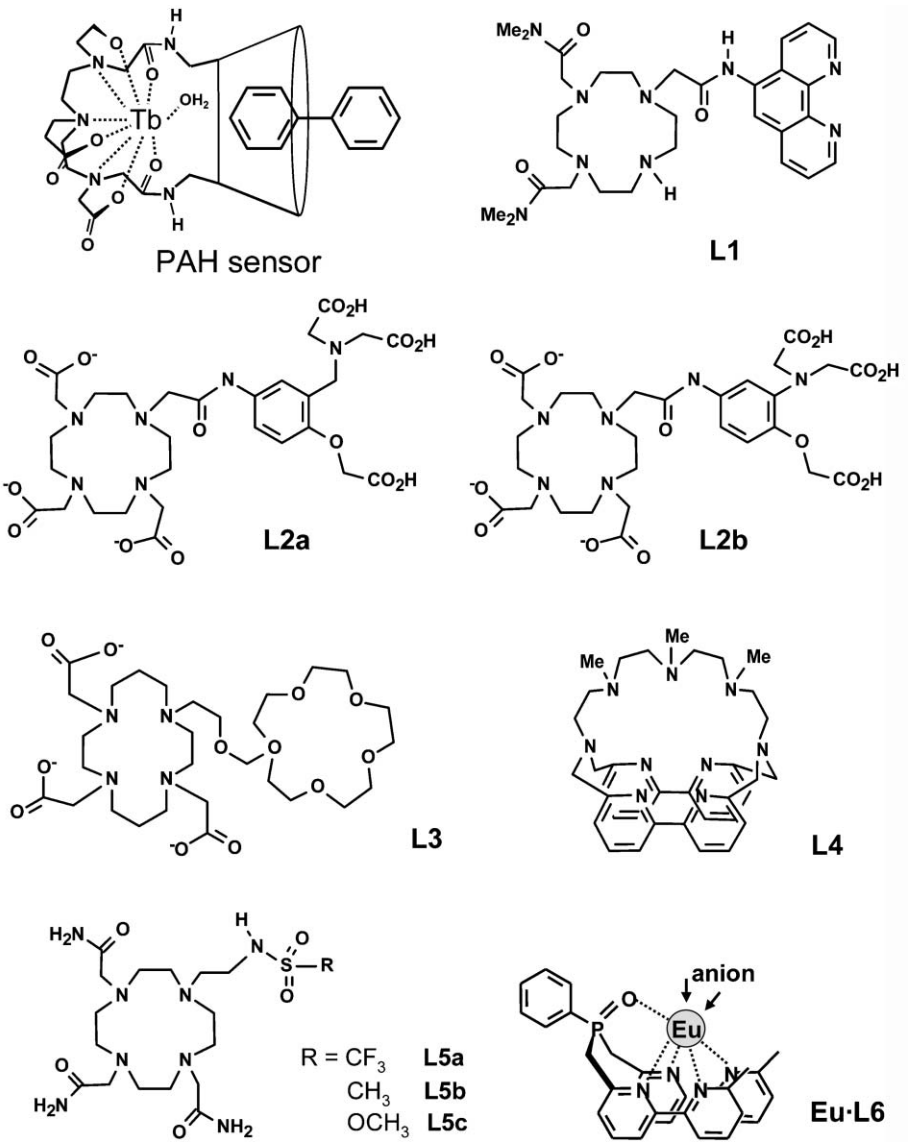

Scheme 1

phenanthroline group acts as a copper chemosensor. Its hydration state is $q \approx 1$ and the emission intensity is pH-sensitive in water, going through a maximum at physiological pH 7.4. At that pH, **Eu·L1** reacts with Cu^{II} to yield a tetrametallic species [Cu(**Eu·L1**)$_3$] in which $^5D_0$(Eu) luminescence is extinguished because the presence of the 3d-transition metal quenches the phen S_1 state by electron transfer, annihilating subsequent energy transfer onto the 4f cation. Europium luminescence is restored upon destruction of the copper complex by addition of edta. Because of this quenching mechanism, Zn^{II} and group I and II cations do not modulate Eu^{III} emission. Moreover, Cu^{II} is selectively detected over Co^{II} and Fe^{II} and binding of Cu^{II} occurs in a narrow concentration range (pCu = 5–6), corresponding to the physiological concentration of this cation.[69]

Pentadentate ligand systems containing aniline or benzylamine nitrogen atoms covalently linked to a kinetically stable Eu or Tb complex, **Ln·L2a** and **Ln·L2b** (Scheme 1) have been synthesized for designing M^{II} luminescent sensors. Covalent linkage to the dota complexes does not alter significantly the affinity for the M^{II} ions (and leave unchanged the affinity sequence) compared with the parent pentadentate ligands, nor does it alter the hydration number ($q = 1$) of the Ln^{III} ions. On the other hand, changes in emission from the Ln excited state accompany M^{II} ion interaction with the luminescent sensors. This allowed determination of Zn^{II} concentrations in a micromolar range, in presence of a simulated extracellular ionic background ($MgCl_2$ 1.16 mM, $CaCl_2$ 2.3 mM, NaCl 140 mM, KCl 4 mM), Tb^{III} emission being enhanced 25% in **Tb·L2aZn** with an apparent dissociation constant of 0.6 μM. The selectivity observed for the binding of Zn^{II} with respect to Ca^{II} and Mg^{II} is in line with Zn^{II} preference for a tertiary N donor; the enhanced Ln luminescence reflects changes in the excited and charge transfer states induced by M^{II} ion binding to aryl oxygen and benzylic nitrogen in **Ln·L2a** and to the aniline N in **Ln·L2b**. A disadvantage of this system is the excitation wavelength needed, which lies in the UV-range (262 nm), while bioanalyses are more sensitive when the

excitation wavelength is larger than 350 nm, avoiding excitation of background luminescence from the biological molecules.[70]

Crown ethers are ideal macrocycles for the selective complexation of alkaline cations and several luminescent complexes fitted with pendant crown ethers have proved to be efficient chemosensors for these ions like for instance the K^I sensor proposed by de Silva and based on photo-induced electron transfers.[71] Other signalling systems take advantage of lanthanide complexes with cyclam (1,4,8,11-tetraazacyclotetradecane) fitted with either a 15-crown-5 or an aza-15-crown-5 pendant arm. The luminescence lifetimes of **Tb·L3** (Scheme 1) in water and deuterated water reflect a hydration state $q = 1$ in absence of alkali metal in the solution, pointing to co-ordination of the ether function of the linking arm. When sodium is added, its complexation to the macrocycle pendant arm and possibly to carbonyl groups of the cyclam moiety generates a steric hindrance which blocks the 9th coordination site and, as a result, the lifetime of $^5D_4$(Tb) increases considerably (from *ca.* 1.8 to *ca.* 3 ms), reflecting $q = 0$. The system is therefore useful for signalling Na^I cations; it responds equally to K^I and, to a much smaller extent, to Li^I.[72]

pH sensors. pH is an essential parameter of physiological processes which very often operate within a very narrow pH range; typical examples are enzymes the activity of which is switched on or off depending on the pH. It is therefore natural that many pH sensitive luminescent signalling systems have been developed, some of them based on Ln^{III} emission. For instance **Eu·L1** displays a bell-shaped change in luminescence intensity upon pH variation from 1.5 to 12, with a maximum around pH 6. In fact, in alkaline solution, Eu^{III} is reduced to Eu^{II} by a photo-induced electron transfer, while in acidic solution, protonation of the phenanthroline amine groups increases the oxidation potential, and leads to a decrease in the isc efficiency, henceforth reducing the ability of the antenna to populate the Eu(^5D_J) levels.[73] Similarly, the water-soluble cryptate [Eu ⊂ **L4**]$^{3+}$ features highly pH-dependent luminescent properties. Lifetime measurements are consistent with hydration states $q \approx 2$ at pH 2 and $q \approx 1$ at pH 6.8. Protonation of the amine functions of the polyamine chain indeed prevents co-ordination onto the metal ion, allowing water molecules to bind in the inner co-ordination sphere. The luminescence intensity remains small up to pH 5 and then increases sharply with a maximum at pH 7. The emission intensity then decreases at basic pH values due to the formation of hydroxylated species [Eu(OH)$_n$ ⊂ **L4**]$^{(3-n)+}$ ($n = 1,2$).[74] Variable hydration state with a switching between $q \approx 2$ and $q \approx 0$ is also the basis of the pH-controlled modulation of luminescence intensity in substituted dota complexes **Eu·L5**. Here the relative emission intensity presents a sigmoid variation with pH, with an inflexion point around pH 6.5. In fact, substituent on the arylsulfonamide group allows a modulation of the pK_a (5.7, 6.4 and 6.7 for **L5a**, **L5b**, and **L5c**, respectively). Explanation for the enhanced emission intensity at pH > 6 is similar to the one given for the previous example. More basic pH values result in the deprotonation of the sulfonamide nitrogen which then binds the lanthanide ion, expelling inner-sphere water molecules. Moreover, this binding brings the chromophore closer to the metal ion, resulting in a better sensitization of the 4f-centred luminescence.[75]

Anion sensors. Although somewhat neglected in the development of analytical procedures, many anions have an important biological relevance and efforts have been recently put forward to make anion-controlled luminescent chemosensors available to bio-scientists. Much of these efforts stem from Parker's work, who has investigated the influence of iodide, chloride, bromide, hydrogencarbonate, hydrogenphosphate, sulfate, and lactate on Eu^{III} and Tb^{III} complexes with cyclen derivatives; this work has been recently reviewed.[68] In addition, we would like to present a supramolecular anion sensor which has interesting potential despite its working in acetonitrile only. The **Eu·L6** complex is depicted in Scheme 1, where **L6** is a bis(bipyridine)phenylphosphine oxide ligand. In this complex, the bipyridine fragments act as efficient sensitizing groups while providing together with the phosphoryl group sizeable coordination strength. The co-ordination sphere is however unsaturated, which allows further co-ordination of anions. In the case of nitrate for instance, a first anion expels the solvent molecules while further binding results in the successive de-complexation of the bipyridyl units. Cumulative stability constants ($\log\beta_i$) obtained by spectrophotometric titrations amount to approximately 6, 11 and 14 for the Eu^{III} sensor in acetonitrile. Fluoride, chloride and acetate binding is stronger. The photophysical properties of both **Eu·L6** and **Tb·L6** drastically depend on the nature of the anion in solution; in particular, adding two equivalents of nitrate to a solution of **[Eu·L6](OTf)$_3$** results in a 11-fold enhancement of the metal-centred emission intensity.[76]

2.3 Immunoassays and hybridization detection

The intrinsic advantages of luminescent lanthanide ions, (i) well defined, almost compound-independent emission lines, (ii) large Stokes shift upon ligand excitation and (iii) long lifetime of the emitting state of some Ln^{III} (Sm, Eu, Dy, Tb) combined with high quantum yields obtained upon ligand sensitization in several co-ordination compounds (*e.g.* β-diketonates) have led to the development of time-resolved luminescent immunoassays (Fig. 4) by a small Finnish company (Wallac Biochemical laboratories) located in Turku.[22,23] In time-resolved spectroscopy, excitation occurs *via* a pulsed lamp (or laser) and a time delay is applied before measurement. In this way, the short-lived background luminescence from the organic part of the sample is allowed to fade off before measuring the long-lived metal-centred luminescence, which ensures a better signal-to-noise ratio (Fig. 4a). In addition, since the overall experiment is completed in a few milliseconds, it can be repeated several thousand times during a minute, leading to a very high sensitivity within a few minutes. Finally, the different spectral ranges covered by the emission of Sm^{III}, Eu^{III}, Tb^{III}, and Dy^{III} permit multiple immunoassays to be developed.[23,77] Fig. 5 shows typical emission from these ions in ternary complexes with pivaloyltrifluoroacetonate and 1,10-phenanthroline imbedded in Triton® X-100 micelles for better protection against water interaction; detection limits reached under time-resolved conditions and co-luminescence enhancement by Y^{III}

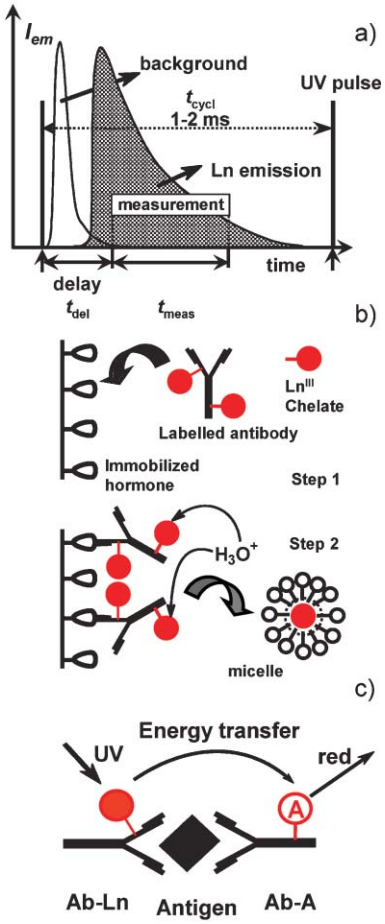

Fig. 4 Principles of (a) time-resolved spectroscopy, (b) heterogeneous immunoassays, and (c) homogeneous immunoassays.

are very low, 3.5×10^{-14} M for Eu^{III} for instance, which is the most sensitive ion under these experimental conditions (Table 2).[78]

Immunoassays rely on a biochemical reaction between an antigen (the analyte) and a specific antibody. In luminescent immunoassays, the latter is labelled with a lanthanide chelate. Initially, the proposed method called for a heterogeneous, two-step procedure (Fig. 4b). The labelling chelate was usually a polyaminocarboxylate complex and after completion of the biochemical reaction (step 1), the solution pH was lowered which resulted in the dissociation of the Ln^{III} ions. Then in

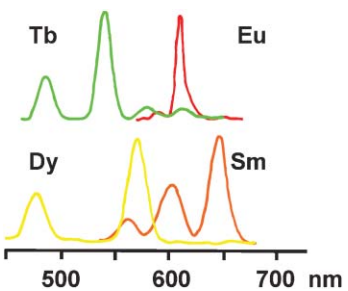

Fig. 5 Emission spectra of ternary lanthanide complexes with pivaloyltrifluoroacetonate and 1,10-phenanthroline, in aqueous solution containing Triton X-100 and Y^{III}.

Table 2 Time-resolved luminescence detection of Ln^{III} (ternary complexes with pivaloyltrifluoroacetonate and 1,10-phenanthroline, aqueous solution with Triton® X-100 and co-luminescence enhancement by Y^{III})[78]

	Experimental conditions (see Fig. 4a)				
Ln^{III}	t_{del}/ms	t_{meas}/ms	t_{cycl}/ms	$\lambda_{em/nm}$	Detection limit/pM
Sm	0.05	0.2	1	644	7.9
Eu	0.5	1.5	2	613	0.035
Tb	0.4	0.5	1	545	0.34
Dy	0.05	0.1	1	573	46

step 2, an enhancement solution was added containing a second chelating agent (usually a β-diketonate), tri-octyl phosphine oxide to complete the Ln^{III} coordination sphere and Triton® X-100 to form protective micelles around the new chelate for optimum luminescence efficiency. In this way, quantum yields of Eu^{III}-containing systems easily reached 70%. A simpler method was subsequently proposed (Fig. 4c) in which the initial chelate is an efficient donor for sensitizing emission of an acceptor chromophore, *e.g.* phycobiliprotein.[79] In such a homogeneous assay, an Eu^{III} complex with a derivatised tris(bipyridine) cryptand (bpy.bpy.bpy in Scheme 2) is linked to a specific antibody while the acceptor is grafted onto a second specific antibody. The biochemical reaction brings the two entities close enough so that directional non-radiative resonant energy transfer occurs upon UV excitation of the chelate. The phycobiliprotein has a high molar absorption coefficient and a specific fluorescence band at 660 nm. The corresponding singlet state is solely populated by the energy transfer process, sometimes referred to as LRET (Luminescence resonance energy transfer), which means that the 660 nm emission reflects the de-excitation decay of the Eu^{III} cryptate or, in other words, that the apparent decay time of the 660 nm fluorescence is identical to the lifetime of $Eu(^5D_0)$ and time-resolved technique can be applied. Energy is only transferred when the donor and the acceptor lie at a relatively short distance so that it only occurs when both antibodies are connected onto the substrate. Therefore, there is no need to eliminate unreacted reagents from the solution before measurement, henceforth, a simplified and faster method. For instance, prolactin can be detected with a sensitivity similar to the one obtained with radioactive labels, down to 0.3 μg per litre.

Advances in recombinant DNA technology and sensitive methods for analyzing the organization of specific genes are major contributors to genomics. These techniques rely on nucleic acid hybridization probes for detecting complementary nucleic acid sequences and are being increasingly used in diagnostic medicine. Several systems have therefore been proposed for detecting protein hybridization by a time-resolved luminescence procedure identical to the one described for homogeneous immunoassays, but using different lanthanide chelates (often polyaminocarboxylates) and acceptors (cyanine dyes). A typical example is illustrated on Fig. 6. A single stranded DNA is fitted at its 5′ end with a europium chelate derived from a carbostyril dye, while the energy acceptor cyanine-5 dye is linked to another single stranded DNA. Upon hybridization, the donor and acceptor are

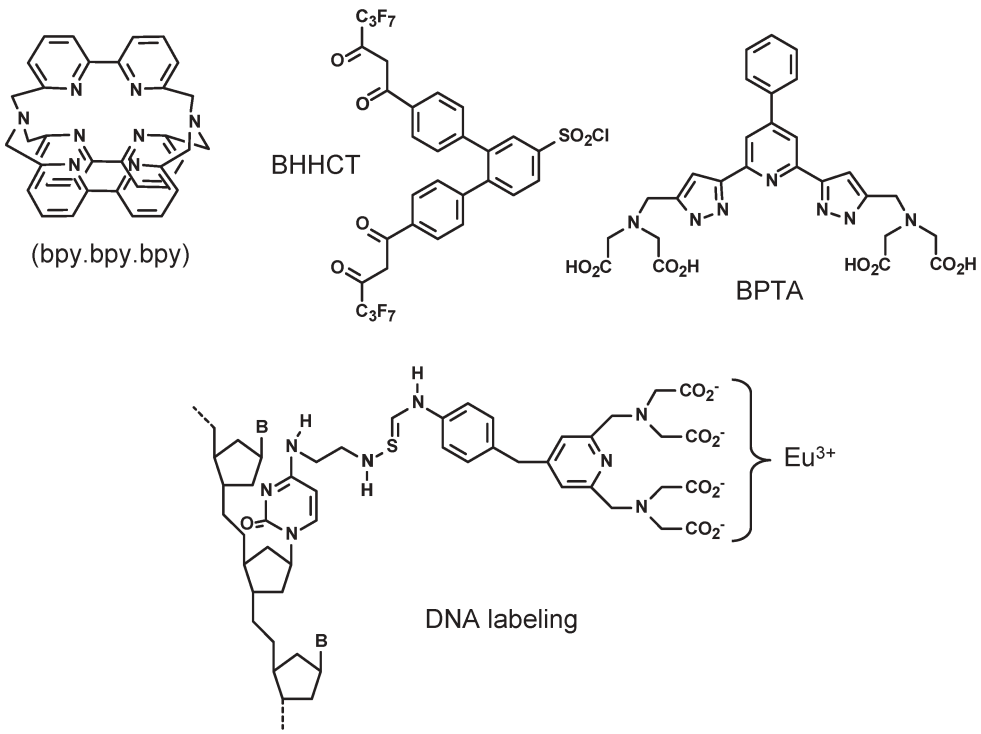

Scheme 2

brought within adequate distance and energy is directionally transferred onto the latter when the donor is excited by UV-light, henceforth allowing detection and quantification of the hybridization process. Chemical labelling of DNA has been achieved in several different ways, one of which is given in Scheme 2: deoxycytidine residues of DNA are transaminated in the presence of ethylenediamine and the resulting compound is reacted with a Eu^{III} chelate, yielding the depicted labelled DNA; the transamination reaction can be adjusted to tune the desired degree of labelling.[80]

Alternatively, homogeneous immunoassays may take advantage of highly luminescent europium chelates[12] and a very efficient system has been proposed by Matsumoto *et al.* who demonstrated its potential in the case of the analysis of human immunoglobulin E (I_gE), which is related to various allergies.[81] The bifunctional ligand 4,4′-bis(1″,1″,1″,2″,2″,3″,3″-heptafluoro-4″, 6″-hexanedion-6″-yl)-chlorosulfo-*o*-phenyl (BHHCT, Scheme 2) bears one chlorosulfonyl group for coupling with proteins and its Eu^{III} complex displays a sizeable stability and quantum yield. It can be easily coupled to streptavidin A (SA), bovine serum albumin (BSA) or both to enhance its solubility. The human I_gE assay is depicted on Fig. 7. A first anti human I_gE antibody (from goat or rabbit) is incubated in the wells of a microtiter plate. The I_gE analyte is then incubated in the coated wells, followed by the incubation of a second biotinylated anti human I_gE antibody, also of animal origin. Finally, the immunoassay is conducted with either the SA or the BSA–SA conjugates of the BHHCT chelate. Astounding results were obtained: the assay lasts only a few hours, its reproducibility is excellent, and its sensitivity is down to 3.6 pg cm^{-3}, which translates into the detection of *ca.* 10^{-18} mol. As a comparison, conventional assays using ELISA (enzyme linked immunosorbent assay) are 10–100 times less sensitive and last 10–20 times longer. Several other assays have been proposed which use the BHHCT ligands and more stable chelates have also been designed with BPTA (Scheme 2) for the

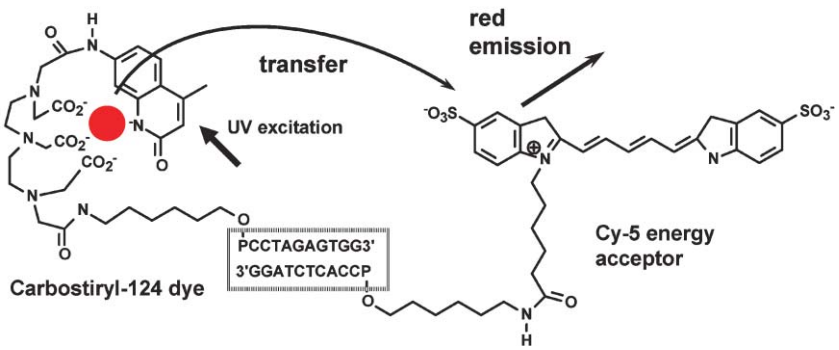

Fig. 6 Detection of hybridization by luminescence resonant energy transfer (LRET).

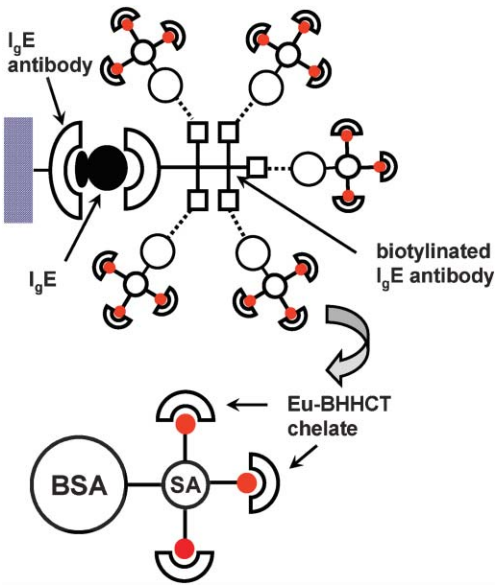

Fig. 7 Principle of the I_gE luminescent immunoassay.[81]

same purposes. Multiple components assays (*e.g.* with several different Ln^{III} ions) are becoming increasingly common for the simultaneous analysis of several analytes and moreover, cell activity can also be monitored by these procedures.[12]

2.4 Imaging techniques

Adding a second or third dimension to analytical procedures offers obvious inherent advantages and luminescence microscopy has therefore become commonplace since suitable detectors have become available. In this context, lanthanide luminescence provides further benefit by adding time-resolved capability which allows one to eliminate scattered light and short-lived fluorescence from cytochemical samples and optical components.[14] Interestingly, and to our knowledge, one of the first practical applications of lanthanide time-resolved imaging dealt with detecting latent fingerprints for forensic purposes.[82] Instrumentation is relatively simple since time-gated experiments eliminate the need to divert the excitation beam; a simplified scheme of the instrumentation used by Vereb *et al.* in their systematic investigation of the experimental parameters[83] is shown on Fig. 8. The microscope allows simultaneous recording of time-resolved and spectrally-resolved images. The intermittent light source is either a chopped light beam, a fast (microsecond) pulsed xenon lamp or a pulsed laser. The filter block contains an excitation filter, a dichroic mirror and an emission filter selected according to the luminescent probe; the time-resolved system is made of a gated, modulated microchannel plate intensifier and a cooled, slow-scan charge-coupled device camera. The instrumentation was successfully tested with a Eu^{III} polyaminocarboxylate derived from dtpa, **Eu·L7** (Scheme 3) which proved to be an excellent luminescent probe for dual temporal and spectral resolution. Introduction of additional polarization optics enables the determination of emission polarization which reflects molecular orientation and rotational mobility, henceforth the nature of the microenvironment sustained by the

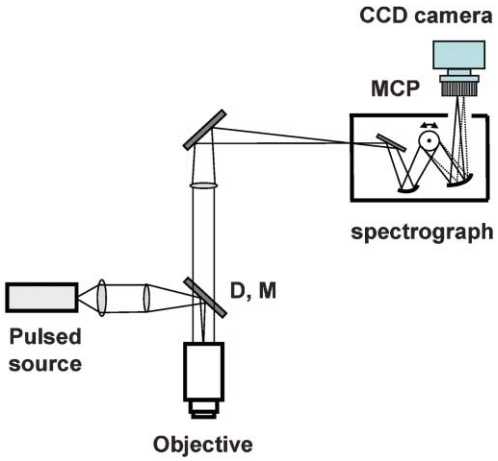

Fig. 8 Schematic diagram of a time-gated luminescence microscope allowing time and spectral resolution of images; D, M = filter block with a dichroic mirror, MCP = gated/modulated microchannel plate intensifier. Adapted from ref. 83

luminescent probe. Several other luminescent markers for microscopy purposes have been proposed by other research groups (Scheme 3). One may divide them into two groups, one relying on visible emission from Eu^{III} and Tb^{III} and the other on near infrared (NIR) luminescence mainly from Yb^{III}. In any case, selective targeting is always desired and efforts concentrate often on the imaging of cancer cells.

Complexes with macrocycles **L8**[84] and **L9a**[85] belong to the first group and have been synthesized in an effort to obtain tissue-selective luminescent probe for imaging cancer cells. In particular, it is hoped that **Tb·L9a**·could be used to help identify early-stage oral cancer lesions.[85] Eu^{III} and Tb^{III} complexes with **L10** are highly luminescent and can be easily coupled to bovine serum albumin (BSA) with labelling ratios up to 8 (Ln : BSA), making them suitable for time-resolved microscopy.[86] Similarly, europium chelates with cyclen derivatives **L11** and **L12** can be used to label silica particles and generate time-resolved images of them.[87] Interest in dual probes, generating both a MRI and a luminescent signal is growing. Indeed, usual brain tumour imaging by MRI is often limited because of the indirect reach of the method; in particular, it sometimes fails to delineate very precisely the boundaries of the tumour. An ideal tumour imaging reporter would therefore, in addition to being tumour specific, provide a luminescence signal which can be correlated with the magnetic resonance. Chelating agent **L9b** is adequate for this purpose and Bornhop's group have coupled it with a tumour specific benzodiazepine receptor and the Eu^{III} complex of the resulting trifunctional ligand displays a bright luminescence in micromolar solutions as well as a good MRI contrast capability. They have obtained convincing results in bimodal imaging of C6 glioma cells from a brain cancer.[88]

Fascinating developments are taking place to overcome some of the limitations inherent in the previously described luminescent probes, namely the facts that (i) the visible emitting Ln^{III} ions usually require UV excitation, which compromises *in vivo* applications since bio-molecules usually absorb heavily in this spectral range and, moreover, biological

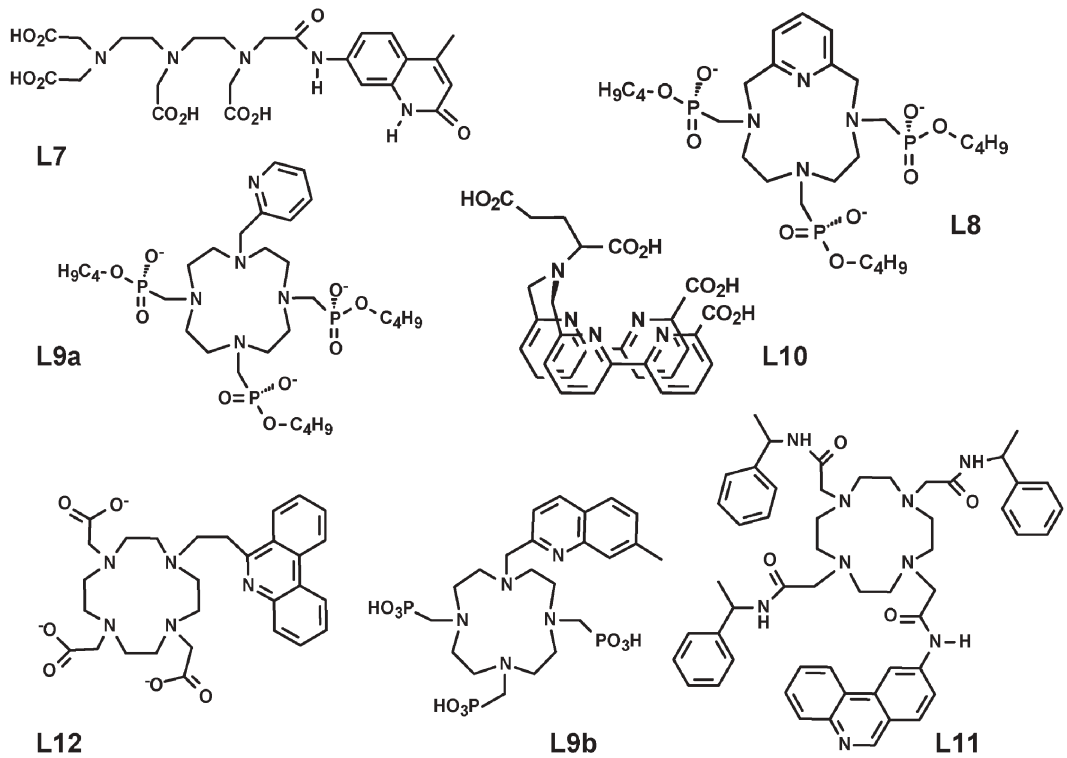

Scheme 3

activity can be modified or destroyed by UV radiation, and (ii) if generated inside a bio-material, visible light may also be substantially absorbed, reducing the signal from the analyte. One solution is to turn to NIR emission since biological tissues are rather transparent in this spectral range. For instance, a water-soluble Yb^{III} porphyrin–BSA conjugate has been proposed for studying lipid membranes;[89] it displays, however a relatively low quantum yield, 0.18%, a figure which is difficult to increase in view of the small energy gap between the $^2F_{5/2}$ and $^2F_{7/2}$ levels. The relatively short lifetimes of the excited states of the NIR-emitting Ln^{III} ions is a potential disadvantage; however, strategies have been proposed to extend these lifetimes by populating the Ln^{III} *via* energy transfer from a long-lived excited state of a transition metal ion such as chromium (see below).[40,90]

Another solution is to resort to long-wavelength excitation based on multiphoton excitation, *i.e.* absorption of two or three photons, a process known as up-conversion. Simple lanthanide salts can be excited in this way, for instance, Eu^{III} chloride by two photons (796 nm) and Tb^{III} chloride by three photons (805 nm). This requires however a considerable excitation power (200–300 mW) and the use of a Ti:sapphire laser.[91] The number of photons simultaneously absorbed for a given metal ion depend on the excitation wavelength and power as well as on the nature of the ligand co-ordinated to Ln^{III}. Such phenomena have been demonstrated on several Eu^{III} and Tb^{III} complexes with various ligands such as troponin C, a tryptophan mutant (26W), carbostyril 124, coumarin and anthranilate.[92] Even more interesting is the detection of cell and tissue surface antigens using up-converting phosphors. Submicron phosphor particles can be prepared from Y^{III}, La^{III} or Gd^{III} (non-luminescent) oxysulfides, oxyhalides, fluorides, gallates or silicates, into which are incorporated Yb^{III} ions and a sensitizer ion such as Ho^{III}, Er^{III} or Tm^{III}.[93]

3. New luminescent lanthanide-containing materials

3.1. Metallomesogens

The current upsurge in the design and study of lanthanide-containing mesophases[94] is justified by several potential applications pertaining to both bio-analysis and materials sciences. For instance, lanthanide-containing trichromatic materials emitting narrow bands in the basic colours are employed in lighting devices and displays,[7] and the large magnetic anisotropy of some Ln^{III} ions opens the way to magnetic rather than electric switching in liquid crystalline materials.[94,95] Lanthanide-containing mesophases remained largely scientific curiosities until the mid 1980's,[96,97] when systematic efforts aiming at isolating lanthanide complexes with liquid crystalline properties started to develop.[98–102] Basically, such materials can be obtained either by mixing lanthanide salts[103] and complexes[104] with mesogenic materials, or by synthesising lanthanide complexes with mesomorphic properties. The presently known lanthanide-containing molecular compounds exhibiting liquid crystalline phases belong to four different classes: (i) lanthanide alkanoates, (ii) Schiff base derivatives: for instance, reaction of a derivative of hydroxybenzaldimine with lanthanide nitrates yielded smectic liquid crystals having an unusually high magnetic anisotropy,[99,105,106] (iii) macrocyclic complexes, which were among the first reported lanthanide-containing metallomesogens, and (iv)

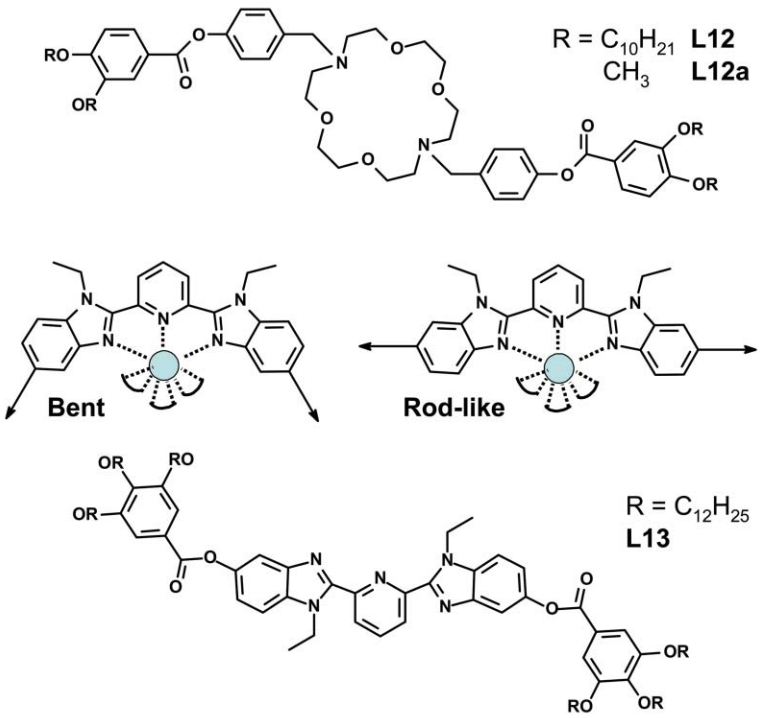

Scheme 4

complexes with tridentate aromatic receptors derived from substituted 2,6-bis(benzimidazoylpyridine). In our laboratories, we have developed synthetic strategies pertaining to the last two categories of compounds[107,108] with the aim of obtaining luminescent metallomesogens. We have also shown how luminescence parameters can be used to detect crystal-to-liquid crystal phase transitions.[109,110]

The design of thermotropic metallomesogens obeys the same rules as those established for the preparation of mesophases with organic molecules. The formation of the liquid crystalline phase corresponds to a thermally induced micro-segregation between the flexible alkyl chains and the more rigid metallic core. Specific molecular shapes usually result from the global anisotropy of the ligands with, in addition, a contribution from the stereochemical requirements of the metal ion. The spherical and bulky trivalent Ln^{III} ions have large co-ordination numbers and no pronounced stereochemical preferences, rendering difficult their introduction into thermotropic mesophases. One strategy implies the use of macrocyclic ligands based on frameworks known to complex lanthanide ions with a reasonable strength. As an example, non-mesomorphic ligand **L12**, derived from 1,7-diaza-18-crown-6 ether, forms mesogenic complexes with Ln^{III} nitrates (Scheme 4). In the case of **Eu·L12**, a combination of differential scanning calorimetry (DSC), polarized light microscopy (PLM) and small angle X-ray diffraction data (SAXS) indicate the formation of a hexagonal columnar mesophase Col_h at 86 °C, while isotropization occurs around 198–200 °C. The temperature range of the liquid crystalline phase can be tuned by varying the counterion and the number of pro-mesogenic alkyl chains grafted onto the ligand.[107] For the Eu^{III} mesomorphic complex **Eu·L12**, in the absence of suitable crystals for structure determination, high resolution luminescence spectra under selective laser excitation yielded a clue to the composition and symmetry of the metal ion environment. In addition, the dependence of both the relative intensity of the hypersensitive $^5D_0 \rightarrow {}^7F_2$ transition, $\ln(I_T/I_{295})$, and of the $Eu(^5D_0)$ lifetime, $\ln(\tau_T/\tau_{295})$, *versus* $1/T$ displays a S-shape curve, allowing a precise determination of the transition temperature (Fig. 9). The decrease in luminescence intensity *versus* increasing temperature of a reference compound **Eu·L12a** not displaying mesomorphic behaviour has also been measured. The emission spectrum of this complex is

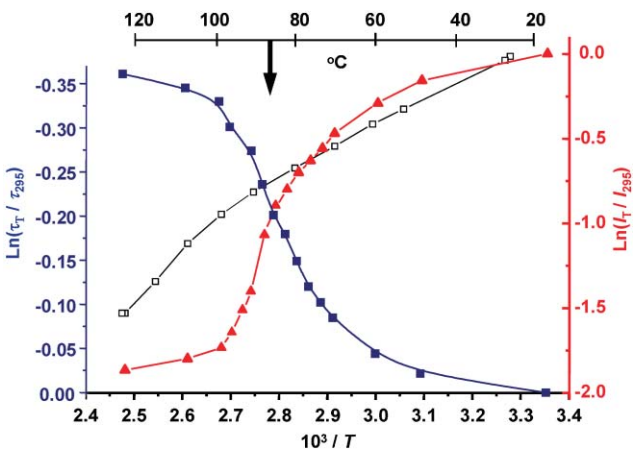

Fig. 9 Integrated and corrected intensities (right scale) of the $Eu(^5D_0 \rightarrow {}^7F_2)$ transition of **Eu·L12** (▲) and **Eu·L12a** (□), and $Eu(^5D_0)$ lifetime (left scale) of **Eu·L12** (■) *versus* temperature. The downward arrow points to the Cr–Col_h transition temperature determined by DSC.

very similar to the luminescence spectrum of **Eu·L12**, but the $\ln(I_T/I_{295})$ *versus* $1/T$ curves for this reference compound is monotonous, although not linear. This variation is mainly due to the temperature-dependent non-radiative de-excitation processes which are similar for the two compounds. In the absence of an electronic-based de-activation process such as photo-induced electron transfer (see eqn (5)), an exponential function of the type $y = y_0\ e^{-C/RT}$ is indeed expected for the variation of both the luminescence intensity and lifetime with temperature.[42,111] From a theoretical point of view, the emission intensity of a Ln^{III} ion is expressed as follows:[112]

$$I(J,J') = \frac{64\pi^4\tilde{\nu}^3}{3h(2J+1)}\left[\frac{n(n^2+2)^2}{9}D_{ED} + n^3 D_{MD}\right] \qquad (6)$$

where $I(J, J')$, in s^{-1}, represents the probability of spontaneous emission, $\tilde{\nu}$ is the average energy of the transition (cm^{-1}), h is Planck's constant (6.63×10^{-27} erg s), $(2J+1)$ is the degeneracy of the initial state (1 for $Eu(^5D_0)$), while D_{ED} and D_{MD} (in $esu^2\ cm^2$) are the contributions from the electric and magnetic dipole operators, respectively, and n is the refractive index of the medium, which is known to undergo a non-linear, S-shaped variation over phase transitions. Since the $^5D_0 \rightarrow {}^7F_2$ transition is purely electric dipole in nature, the second term vanishes and grouping all the constants yields the simplified relationship:

$$I(0,2) = \frac{n(n^2+2)^2}{9} \times D_{ED} \times \text{cst} \qquad (7)$$

The correction factor $\frac{n(n^2+2)^2}{9}$ estimated by measuring n over the temperature range of the mesogenic phase transition of **Eu·L12** is relatively small and contributes to a maximum of 15% to the $I(^5D_0 \rightarrow {}^7F_2)$ variation, so that the drop observed at the transition temperature (Fig. 9) is genuine to the phase transition. It is noteworthy that both the intensity and lifetime variations are reversible and reproducible over many heating–cooling cycles. A similar effect has also been observed for **Tb·L12**, as far as the intensity of the $^5D_4 \rightarrow {}^7F_5$ transition is concerned. Consequently, luminescence intensity and/or lifetime switching can be used to signal Cr–LC transitions in Eu^{III} and Tb^{III} mesomorphic compounds.

Another way of producing Ln-containing mesogenic compounds is the introduction of the Ln^{III} ions into a cavity induced by suitable ligand(s) and displaying rod-like or disk-like anisotropy,[94] a reason why we have developed semi-rigid aromatic tridentate ligands for which rod-like or bent geometries depend on the position of the lipophilic residues; these two basic shapes interconvert upon complexation with lanthanide nitrates, yielding the two situations depicted in Scheme 4.[108] Ligand **L13** for instance, which bears spacers in 5,5′ positions playing the role of sensitizing units for Eu luminescence, corresponds to the rod-like situation. It possesses mesomorphic properties by itself and its associated bent luminescent complex with europium nitrate **Eu·L13** features liquid crystalline behaviour at elevated temperature with a cubic phase between 140 and 200 °C. Again, the strong red europium-centred photoluminescence of this metallomesogen can be exploited for extracting thermal and structural information of the phase transition. High-resolution investigation shows **Eu·L13** being comprised of a single metal ion site and the near constancy of the $Eu(^5D_0)$ lifetime between 10 and 295 K is indicative of weak coupling with high energy vibrations. Plots of $\ln(I_T/I_{295})$ and of the $\ln(\tau_T/\tau_{295})$ display sigmoid variation when **Eu·L13** enters its cubic mesophase during the first heating process, reflecting structural changes induced by the Cr–Cub process. However, subsequent cooling and heating–cooling cycles reveal that the organization in the Cub phase is supercooled in the final glassy state and the $\ln(I_T/I_{295})$ and $\ln(\tau_T/\tau_{295})$ plots are almost monotonous, the residual small curvature being attributable to the refractive index change.[108]

Other luminescent and mesogenic Eu^{III} molecular compounds have been reported by Binnemans and Galyametdinov. For instance, lanthanide complexes derived from 4-dodecyloxy-*N*-hexadecyl-2-hydroxybenzaldimine and perfluorinated alkyl sulfate counterions show a smectic A mesophase. A large increase in the magnetic susceptibility was observed at the isotropic-to-mesophase transition in an applied magnetic field of 1.5 T. The magnitude of the magnetic anisotropy depends on the strength of the crystal field around the metal ion, more precisely on the values of the second-rank crystal field parameters B^2_q. Since in addition to this interesting magnetic behaviour, the Eu^{III} complex is quite luminescent, it was used as a probe for unravelling the crystal field splitting: the magnetic dipole allowed transition $^5D_0 \rightarrow {}^7F_1$ exhibits three components reflecting an unusually large crystal field splitting of the $^7F_1$ level (156, 522, 552 cm^{-1}) corresponding to a very large B^2_0 parameter (1170 cm^{-1}).[106,113] Lanthanide β-diketonates are highly luminescent[48] and complexes in which the 1,3-diphenyl-1,3-propanedionate ligands are substituted in the *para* position by alkoxy chains have been reacted with Lewis-bases; these ternary adducts exhibit monotropic smectic phases and photoluminescence of the Eu^{III} complex is particularly intense at room temperature.[114]

The design of molecular metallomesogens often involves a large synthetic effort to produce the adequate pro-mesogenic ligands, so that another route has been explored, which appears to be simpler. It consists of doping luminescent lanthanide salts or complexes (often β-diketonates) into known room-temperature mesophases.[96,115,116] Luminescence switching has been observed at the nematic-to-isotropic transition of 4-pentyl-4′-cyanobiphenyl (5CB) containing Eu^{III} β-diketonates, the larger emission intensity in the liquid crystalline phase being attributed to better excitation of the sample through large internal scattering of the excitation light.[104] Work is also focusing on obtaining near infrared luminescence (Nd^{III}, Er^{III}, Yb^{III}, see section 3.3), for instance in the nematic host matrices *N*-(4-methoxybenzylidene)-4-butylaniline (MBBA) and 5CB.[117] In our laboratories, we have taken advantage of the mesogenic properties of an ionic liquid presenting a liquid crystalline behaviour at room temperature, 1-dodecyl-3-methylimidazolium chloride ($[C_{12}$-mim]Cl). This salt form lamellar, sheet-like arrays in the crystalline phase and an enantiomeric smectic liquid crystalline phase at temperatures higher than 0–20 °C depending on its water content. Introduction of lanthanide salts into this ionic liquid does not much alter the liquid crystalline properties and the emission colour of the Eu^{III}-containing material can be tuned from blue

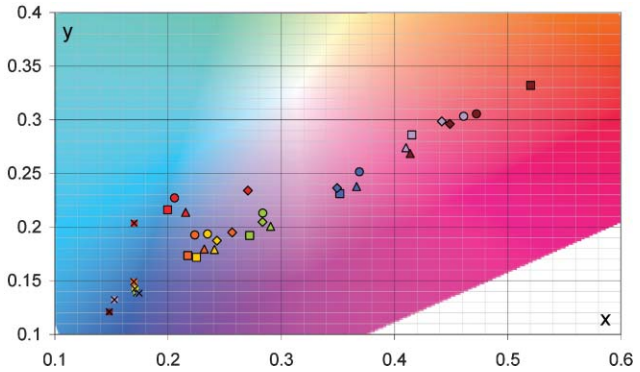

Fig. 10 Trichromatic diagram displaying the position of the studied samples in function of their composition (☒: ionic liquid, ■: chloride, ♦: nitrate, ▲: triflate, ●: perchlorate) and the excitation wavelength (grey: 274 nm, violet: 285 nm, blue: 334 nm, green: 344 nm, yellow: 353 nm, orange: 361 nm, red: 393 nm). Reproduced with permission from ref. 103.

to red by varying the excitation wavelength and the counterion (Fig. 10).[103]

3.2. Lanthanide luminescence in ionic liquids

Room temperature ionic liquids (RTILs) are usually composed of an organic cation (alkylammonium, alkylphosphonium, imidazolium, pyridinium, isoquinolinium) and an inorganic anion (Scheme 5), although chloroaluminates are also a class of RTILs. They remain liquid over a wide temperature range, including room temperature. The first such compounds were reported in 1914,[118] but apart for studies on chloroaluminates in the 1960's for their use as electrolytes in batteries, significant literature has only become available in the late 1980's when their potential as solvents for synthesis, catalysis, and extraction processes was recognized, in view of their extremely low volatility. The anion is often a relatively poorly co-ordinating entity, such as Tf_2N ([bis(trifluoromethane)-sulfonyl]imide) so that besides being highly polar, RTILs can be considered as being non-coordinating solvents, an asset for studying the coordination chemistry of metal ions.[119] In the absence of other donor molecules, Tf_2N^- will of course interact with the metal ion; its co-ordination chemistry is rich in that it presents a range of binding modes, from mono-dentate with metal–O or metal–N bonds, to bidentate η-N,O or η-O,O or, possibly bridging. The earlier studies involving RTILs have been hampered by the high cost of these chemicals and, also, by the fact that they tend to be highly hygroscopic

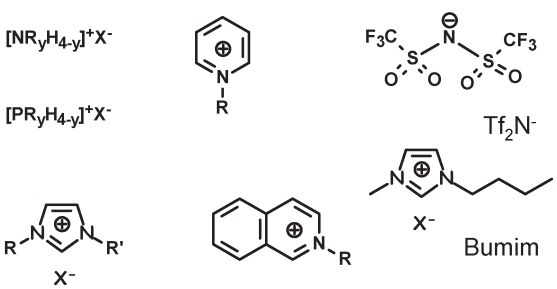

Scheme 5

with physico-chemical properties varying substantially with the water content.[120] However, new synthetic methods are now at hand, which make RTILs more easily available in large quantities.[121] Their physical properties are perfectly known and listed[122] and adequate purification and handling ensure reproducible results.[123] As far as 4f-elements are concerned, initial studies focused on proving the formation of $[LnCl_6]^{3-}$ in aluminium chloride–1-methyl-3-ethylimidazolium chloride mixtures by spectophotometry;[124] moreover, chloro complexes in other RTILs have been the subject of several theoretical studies.[125] The properties of RTILs are easily tuneable, either by modifying the side chains on the imidazolium cation, or by using different anions, a reason why they are now provided in the separation and extraction of 4f and 5f ions.[126] An interesting point for extraction studies is the demonstration that $[Ln(tta)_4]^-$ (tta = 2-thenoyltrifluoroacetonate) is the only species forming in a biphasic aqueous-RTIL mixture, instead of the solvated complexes $[Ln(tta)_2(H_2O)_2]$.[127] This is ascertained by the observation of a single component in the $Eu(^5D_0 \rightarrow {}^7F_0)$ transition as well as by the hydration number $q \approx 0.1$–0.2 determined by measuring the $Eu(^5D_0)$ lifetime in water and deuterated water. On the other hand, EXAFS and HES (extended X-ray scattering) data suggest that the presence of $[Ln(tta)_4]^-$ does not significantly alter the structure of the RTIL. Another study on the complexation of lanthanide ions in a RTIL involved divalent europium iodide which proved to be unusually stable in $BumimPF_6$;[120] spectrophotometric evidences point to the interaction between Eu^{II} and 15-crown-5 ether.

The apparent facile abstraction of water molecules from the inner co-ordination sphere in RTILs may be an advantage for light emission in diminishing non-radiative de-activation processes, so that the photophysical properties of Ln-containing RTILs are starting to be investigated (see also previous paragraph). In a recent study, we have determined the spectroscopic properties of Eu^{III} triflate (trifluoromethanesul-fonate) dissolved in $BmimTf_2N$. When the RTIL is not degassed, that is when it contains an appreciable amount of water, the luminescence decay of the $Eu(^5D_0)$ level is a single exponential function and the corresponding lifetime (0.16 ms) reflects the presence of several water molecules in the inner co-ordination sphere. Upon removal of water, the lifetime increases and the decay becomes eventually bi-exponential with a long component (2.56 ms) suggesting the presence of an anhydrous species. Addition of tetrabutylammonium chloride to the anhydrous solution leads to the formation of a polychloro species, most probably $[EuCl_6]^{3-}$ since the corresponding spectroscopic properties match those obtained in ethanol for this species; in particular the Cl-to-Eu ligand-to-metal charge transfer state is located at 33 000 cm^{-1} and excitation into this state results in $Eu(^5D_0)$ emission.[123] Many ionic liquids are colourless and optically transparent over a wide spectral range, from UV (≈ 220 nm) to NIR (≈ 2000 nm); this, together with their good chemical stability, makes them interesting solvents for optical studies and, potentially, for the design of optically relevant materials in the visible and NIR range. The behaviour of Nd^{III} salts and complexes in 1-ethyl- and 1-hexyl-3-methylimidazolium ionic liquids (counterions: bromide, tosylate or triflate) shows that

sizeable NIR luminescence can be obtained when either neodymium bromide or thenolytrifluoroacetonate is used.[128] Another study demonstrates that intense NIR emission can be observed when carefully dried 1-dodecyl-3-methylimidazolium bis(trifluoromethylsulfonyl)imide is used as solvent for Nd^{III} and Er^{III} iodides. A quantum yield of 2.5 $\pm$ 0.2% was obtained for the Nd^{III} salt, with a lifetime of the $Nd(^4F_{3/2})$ level of 15.3 μs. On the other hand, traces of water readily quench the NIR luminescence.[129]

3.3. Near-IR emitting materials and edifices

As mentioned several times in the preceding sections, lanthanide-based NIR luminescence is attracting considerable interest both in the fields of light emitting diodes, telecommunication, and medical applications in view of their potential for non-invasive *in vivo* imaging. Recently, there have been attempts to use NIR tomography to examine deep tissues, with the idea of developing highly sensitive methods for early detection of cancer.[130] In this respect, receptor-targeted optical imaging of tumours is gaining in interest because haemoglobin has low absorption coefficients above 650 nm, while the absorption of water, a major component of biological tissues, diminishes drastically below 1300 nm. Sensitivity of the luminescent probes can be enhanced in two ways. Firstly by using quenched precursors that can be activated *in vivo* by a suitable biochemical reaction,[131] and secondly, by taking advantage of time-resolved luminescence measurements to separate the probe luminescence from the unwanted background luminescence. NIR-luminescent Ln^{III} ions such as Nd^{III} or Yb^{III}, although potentially interesting in view of their emission wavelengths, have two intrinsic drawbacks: (i) low sensitization of the metal-centred luminescence due to a small energy gap between their excited and ground-state levels, favouring efficient non-radiative processes, and (ii) relatively short lifetimes (ns to μs), which limit the efficiency of time-resolved detection. The latter limitation can be overcome by introducing the Ln^{III} ion into a 3d–4f bimetallic edifice in which population of the Ln^{III} excited state is controlled by a long-lived emitting Cr^{III} ion (see section 4). The number of articles dealing with NIR-emitting lanthanide-containing systems has been growing exponentially during the last few years (more than 100 papers have appeared in scientific journals during the last three years) and it is out of the scope of this review to give a detailed account of them. Several classes of materials have been tested and we shall only briefly point to selected examples. A recent review describes suitable strategies for the fabrication of devices containing Nd^{III}, as well as Eu^{III} and Tb^{III} ions.[132]

Purely inorganic systems are still praised in optical applications, particularly as amplifiers for waveguides in which Al_2O_3 is doped with Er^{III} and Yb^{III}, the later playing the role of sensitizer for the former and therefore allowing excitation in the NIR range, at 980 nm for which cheap laser diodes exist.[133] Surface-coated nanoparticles of lanthanum fluoride and phosphate doped with luminescent Ln^{III} ions have been proposed. In these systems, the lifetimes of the emitting Ln^{III} ions is increased by orders of magnitude compared to those commonly observed in organic complexes, with values as high as 1 ms for Er^{III} and 200 ms for Nd^{III}, indicative of a very efficient shielding from non-radiative de-activation processes.[26] Hydrothermal synthesis of layered silicates of general formula $K_3[M_{1-x}Ln_xSi_3O_8(OH)_2]$ with M = Y, Tb and Ln = Eu, Tb, Er resulted in the isolation of materials that proved to be effective room-temperature NIR (Ln = Er) and visible (Ln = Eu, Tb) phosphors with outputs comparable to standards used in commercial lamps. The layered structure of these materials allows the introduction of a third Ln^{III} ion and, henceforth, the fine-tuning of their luminescent properties.[134] Another group of compounds feature organic–inorganic hybrids, either coordination polymers, many of them being obtained by hydrothermal reactions,[135] or polymers blended with lanthanide complexes. Several of these systems are optimized for electroluminescence and used in the fabrication of organic light emitting diodes (OLEDs).[136] In order to minimize de-activation processes, Hasegawa has proposed methacrylate polymers including Nd^{III} ions co-ordinated to tris(bis-perfluoromethane) (or ethanesulfonylaminate) and deuterated dmso; the quantum yields obtained (in the range 1.3–1.6%) are among the largest reported for Nd^{III}-containing polymers.[137] Calcein and dipicolinate complexes have been introduced into silica–polyethyleneglycol hybrids at neutral pH, resulting in strong NIR luminescence from Nd^{III}, Er^{III} and Yb^{III}.[138] Tetraphenylporphyrins are good sensitizers for Ln^{III} NIR luminescence[139] and monoporphyrinate complexes have been inserted into various conjugated and non-conjugated polymers, yielding materials suitable for light emitting diodes in which the porphyrinate complex acts both as the emitter and the charge-transport medium.[140] Substituted tetraphenylporphyrinates grafted on a tripodal anionic ligand, hydridotris-(pyrazoyl-1-yl)borate, have also been used to sensitize with success the luminescence of Er^{III} and Yb^{III}.[141]

Several dyes are known to emit in spectral ranges appropriate for energy transfer onto NIR-emitting lanthanide ions and a few of them are shown in Scheme 6. They have been either incorporated into ternary complexes or grafted onto platforms such as terphenyl, cyclen, or calixarenes. Enhanced Er^{III} luminescence has been obtained with the ion-associating sensitizer IR5, a dye with large absorption cross section in the visible around 488 nm (S_2) and in the NIR, around 980 nm (S_1). The anionic β-diketonate $[Er(hfa)_4]^-$ (hfa = hexafluoroacetylacetonate) associates with the cationic form of IR5 to yield the ion pair $\{[Er(hfa)_4]^-IR5^+\}$. Energy harvested by the dye flows to the fluorescent $^4I_{13/2}$ excited state of the metal ion through its low lying triplet state centred at 7700 cm^{-1} and possibly through the lowest singlet state located at 9000 cm^{-1} since the lifetime of the $^4I_{13/2}$ is relatively short.[142] In a seminal paper,[143] Hebbink *et al.* have covalently attached fluorescein, eosin, and erythrosin. The dyes are connected to a terphenyl moiety through a β-alanine spacer fitted with an isothiocyanate group (**L14–L16** in Scheme 6); this molecular design allows the sensitizing dye to co-ordinate the lanthanide ion and therefore to be in close proximity so that energy transfer is optimized. The complete photophysical study conducted by the authors sheds light on the delicate balance to be achieved in order to get an efficient luminescent device. It is known that introduction of heavy atoms (from H to Br to I in going from fluorescein to eosin to erythrosine) favours population of the

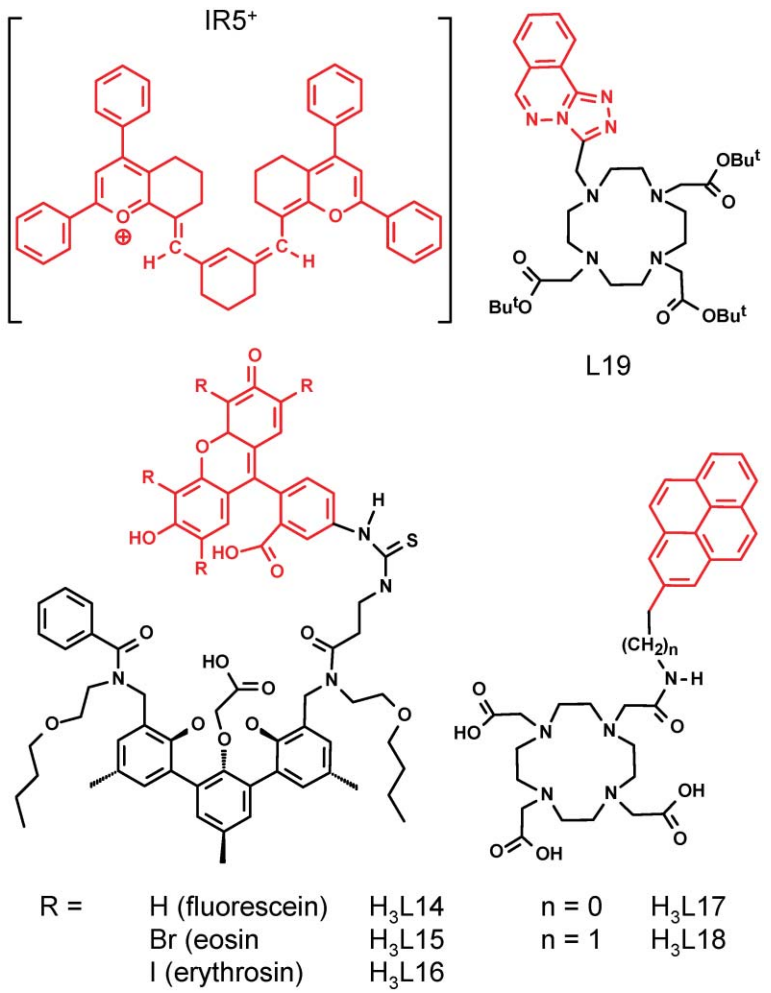

Scheme 6

triplet state by isc, which is effectively observed with $\eta_{isc} = 0.02$, 0.18, and 0.82, respectively. However, complexation with Ln^{III} ions further enhances the isc process and results in less pronounced differences between the three ligands. Since the donor triplet state of $\mathbf{L14}^{3-}$ is at higher energy than those of the two other ligands, less back transfer occurs and, as a result, the complexes **Ln·L14** (Ln = Nd, Er, Yb) display the largest quantum yields. The sensitization efficiencies ($\eta_{isc}\,\eta_{et}$, see eqn (2)) obtained for Nd^{III} and Yb^{III} amount to 0.42 and 0.19, respectively. Absolute quantum yields remain modest, 3×10^{-4} for Nd^{III} and 2.3×10^{-3} for Yb^{III},† mainly because $Q^{Ln}{}_{Ln}$ is very small (see eqn (2)).[143] Using another approach, Faulkner and his group have grafted pyrene[144] and triazolophthalazine[145] onto the cyclen framework. Pyrene is an efficient sensitizer of Nd^{III} and Yb^{III} and it is shown, again, that closer proximity of the sensitizer results in enhanced quantum yields, the ratios between **Ln·L17** and **Ln·L18** being 1.6 : 1. Triazolophthalazine behaves as a good general purpose sensitizer and modulation of its properties is relatively easy in view of the commercial availability of variably derivatised hydralazines.

† Corresponding data for Er^{III} are not available because the $Er(^4I_{13/2})$ lifetime could not be determined.

Another growingly popular sensitizing unit is 8-hydroxyquinoline (**L20–L22** in Scheme 7) which forms several types of complexes with Ln^{III} ions: tris(quinolinates), tetrakis(quinolinates), and trimeric entities Er_3Q_9.[146,147] The feeding triplet state level of quinolinate is situated at 18 000 cm^{-1} and is convenient for populating the $Er(^4F_{9/2})$

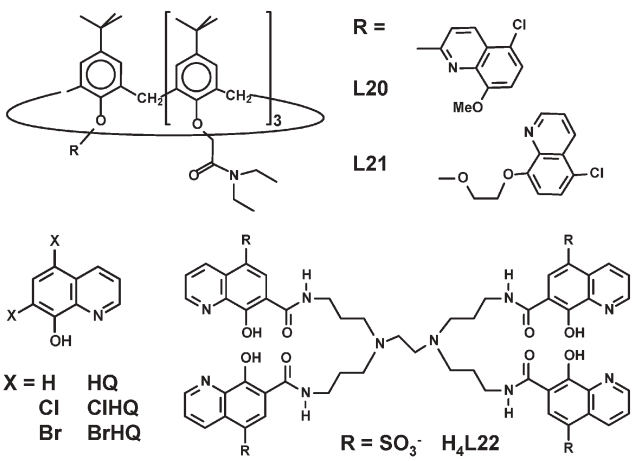

Scheme 7

level; if non-radiative de-activation by high-energy vibrations is prevented, energy will then be transferred onto the fluorescent $^4I_{13/2}$ level. Substitution of quinoline in 5 and 7 positions by chloride or bromide groups increases by about 30% the intensity of the sensitized $^4I_{13/2} \rightarrow {}^4F_{15/2}$ emission, but again the influence of Er^{III} on the isc process is preponderant with respect to the influence of the halogenides.[148] The 8-alkoxy-5-chloroquinoline fluorophore has been covalently linked to a calix[4]arene framework and the resulting ligands **L20** and **L21** bind Ln^{III} nitrates in acetonitrile, a process upon which the fluorescence of the host is quenched and the luminescence of the Ln^{III} ions enhanced (Ln = Nd, Er, Yb).[149] In our laboratories, we have developed a ligand based on 1,2-diaminoethane, fitted with four chromophoric 8-hydroxyquinoline chelating arms (**H_4L22**, Scheme 7), which features pK_as ranging from 1.8 to 12.1. Interaction with Ln^{III} ions is strong and in the pH range 7–9, in which most of the physiologically relevant applications take place, the major complex species is $[Ln(\mathbf{H_2L22})]^{3-}$. In the case of Eu^{III}, a pEu value of 15.6 was obtained, as compared to 19.6 for the standard diethylenetriamine penta-acetate chelate, so that the chelates with **H_4L22** can be envisaged for *in vivo* applications. Most interesting is the fact that in aqueous solution no water molecule coordinates onto the metal ion. Combined with the adequate photophysical properties of 8-hydroxyquinoline, this results in sizeable quantum yields (in water) for the Nd^{III} and Yb^{III} 1 : 1 chelates (Table 3).[150] These figures can even be doubled by introducing a methyl substituent on the amide functions.[151]

4. Controlling luminescent properties in multimetallic assemblies

In the preceding section, we have shown how chemists try to cope with the numerous requirements pertaining to the elaboration of efficient lanthanide-containing luminescent edifices. They usually rely on known stable chelating agents, derivatised with an adequate chromophore. Despite the large variety of systems tested, which illustrates the unlimited imagination of chemists and sometimes led to the elaboration of entire libraries of ligands, these efforts may appear to lack some systematic underlying principles. This is easily explainable in view of the rather intricate energy transfer processes leading to sensitization of lanthanide luminescence, in which broad-band and short-lived excited states from the ligands have to interact with narrow and long-lived metal-ion states. Despite valuable efforts,[29–31] theory is not developed enough to ensure reliable predictions yet. Another, more controlled approach is to resort to intermetallic communication between two (or more) metal ions inserted into polymetallic edifices

Table 3 Photophysical properties of the $[Ln(\mathbf{H_2L22})]^{3-}$ chelates 6.2 × 10^{-5} M in water and deuterated water[150]

	H_2O		D_2O	
Cmpd	τ/μs	Q^L_{Ln}/%[a]	τ/μs	Q^L_{Ln}/%[a]
$[Nd(\mathbf{H_2L22})]^{3-}$	0.13 ± 0.01	0.02	0.58 ± 0.02	0.10
$[Yb(\mathbf{H_2L22})]^{3-}$	2.21 ± 0.01	0.18	10.0 ± 0.01	0.81

[a] ±20%

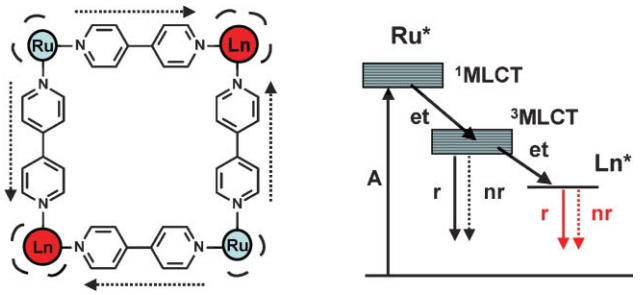

Fig. 11 (Left) Tetrametallic complex exhibiting Ru^{II}-to-Ln^{III} (Ln = Nd, Yb) directional energy transfer; Ln^{III} ions are under the form of $[Ln(tta)_3]$ complexes and Ru^{II} ions are bound to bipyridyl units (redrawn from ref. 152). (Right) Sensitizing mechanism.

such that directional energy transfer is feasible. In this way, one may control the properties of one metal ion by tuning the physicochemical properties of the other ion. This strategy is being mostly used for sensitizing NIR emitting Ln^{III} ions (although this is not a theoretical constraint) and two major options are at hand: through-bond or through-space directional energy transfer. A typical example of the first process is given by the tetrametallic square Ru_2Ln_2 complex proposed by Guo *et al.* (Fig. 11).[152] Divalent ruthenium possesses a metal-to-ligand-charge transfer triplet state located around 16 000 cm^{-1}, which is convenient for populating Nd^{III}, and to a lesser extent Yb^{III}, excited states, as shown on Fig. 11.

The energy of the MLCT states largely depends on the d-transition metal environment and can therefore be tuned by modifying the hosting ligands. An example of the through-space strategy is shown in Scheme 8 for a trimetallic $RuLn_2$ in which the d- and f-transition metal ions are not directly linked by an electronic relay.[153] The latter intermetallic through-space communication is relevant to standard d → f sensitization (or f → d relaxation) programmed in doped ionic crystals for optimizing optical responses.[38,154] Such strategy has been already mentioned when discussing quantum cutting (section 1.1),[21] and it has been recently extended for improving the efficiency of nonlinear up-conversion processes.[155–157] Since this section concentrates on discrete multimetallic systems displaying directional energy transfers, statistical intermetallic communications in doped ionic crystals will not be further considered. For discrete f–f systems, the lack of suitable synthetic methods for producing pure heteropolymetallic complexes prevents the exploitation of directional intermetallic energy transfer processes.[64,158] It is only recently that Faulkner and Pope took advantage of the kinetic inertness of Tb^{III} cyclen macrocycles for producing the neutral pure heterotrimetallic [TbYbTb**L23**], in which convergent intramolecular Tb → Yb energy transfer processes are responsible for the sensitization of the NIR Yb^{III} emitter (Fig. 12).[159]

For d–f systems, the thermodynamic differentiation between the two types of metal ions is easier to achieve, particularly with soft d-block ions, and a plethora of segmental acyclic and macrocyclic ligands have been coded for the selective incorporation of *n*d- and 4f-block ions in discrete molecular architectures.[64,158,160] As far as luminescence is concerned, the rigidification and/or organization of the chromophoric antenna through the coordination of a d-block ion is the most

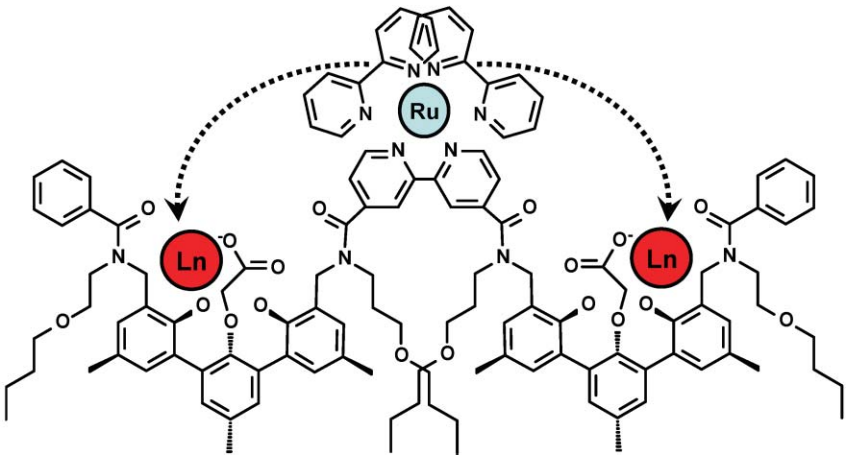

Scheme 8

simple symbiotic function, which may improve the intramolecular sensitization of the f-block partner. The surprising improvement of the Ln-centred emission upon complexation of the closed-shell Zn^{II} ion in $[ZnTb\mathbf{L24}]^{2+}$ (Fig. 13),[161] or in $[ZnEu(\mathbf{L25}\text{-}3H)]^{2+}$ (Scheme 9)[162] has no other origin, but the replacement of Zn^{II} with the open-shell Ni^{II} cation in $[EuNi(\mathbf{L25}\text{-}3H)]^{2+}$ induces a completely different behaviour with the quantitative quenching of the Eu-centred luminescence, which results from an efficient intramolecular Eu → Ni energy transfer. Since we can reasonably assume that the

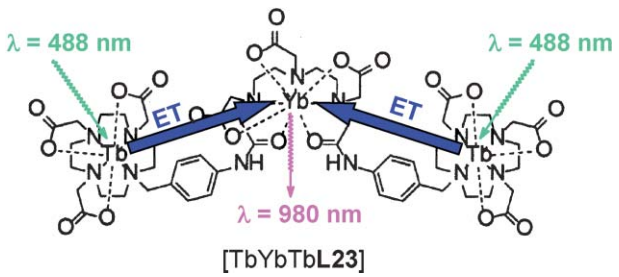

Fig. 12 Schematic representation of the intramolecular f → f energy transfer processes responsible for the sensitizing of Yb^{III} in the heterotrimetallic complex [TbYbTb**L23**].[159]

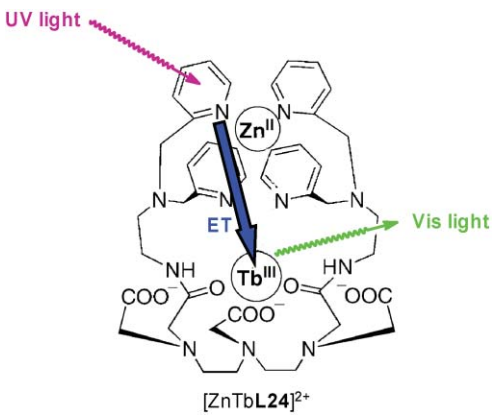

Fig. 13 Schematic representation of the Zn^{II}-induced organization of a polypyridine chromophore for sensitizing Tb^{III} in $[ZnTb\mathbf{L24}]^{2+}$.[162]

Förster dipole–dipolar mechanism dominates intermetallic d↔f communications occurring at 'long' distances (> 4 Å), eqn (4) implies that its efficiency, measured by the distance for 50% transfer (R_0), mainly depends on the overlap integral J between the emission spectrum of the donor and the absorption spectrum of the acceptor. A look at Fig. 1 shows that a large amount of Ln-centred excited states located below 20 000 cm^{-1} (except for Ln = Gd) are amenable to undergo significant overlap with broad d–d or charge transfer (CT) bands characteristic of the d-block chromophores. We can thus predict that R_0 for d–f pairs are often considerable (typically 5 Å $\leqslant R_0 \leqslant$ 20 Å), which implies that (i) quantitative energy transfers occur at short distances, (ii) communications at long distances remain accessible, and (iii) specific modulation of intermetallic energy transfer mainly relies on the manipulation of the d-centred excited states. The latter point is illustrated with the triple helical complexes $[EuFe(\mathbf{L26})_3]^{5+}$ and $[EuFe(\mathbf{L27})_3]^{5+}$, in which the two cations are separated by a fixed distance of 9 Å (Scheme 9).[163,164] When the terminal methyl group is connected to the 5-position of the pyridine ring in $[EuFe(\mathbf{L26})_3]^{5+}$, the violet pseudo-octahedral $[Fe^{II}(benzimidazole\text{-}pyridine)_3]^{2+}$ chromophore preferentially adopts the low spin $^1A_1$ electronic ground state configuration, which displays an intense spin-allowed transition toward a broad ^{1}MLCT excited state, covering a large part of the visible domain (Fig. 14a). Efficient overlap is observed with the emission spectrum ($^5D_0 \rightarrow {}^7F_j$) of the neighbouring Eu^{III}, and a quantitative $Eu^{III} \rightarrow Fe^{II}{}_{ls}$ energy transfer is responsible for the complete quenching of the Eu-centred luminescence (Fig. 14a).[163] The shift of the methyl group to the 6-position of the pyridine ring in $[EuFe(\mathbf{L27})_3]^{5+}$, sterically constrains the orange pseudo-octahedral $[Fe^{II}(benzimidazole\text{-}pyridine)_3]^{2+}$ chromophore to adopt a pure high spin $^5T_2$ electronic ground state configuration, which drastically reduces the spectral overlap with the $^5D_0 \rightarrow {}^7F_j$ emission of the Eu^{III} donor (Fig. 14b).[164] The efficiency of the $Eu^{III} \rightarrow Fe^{II}{}_{hs}$ energy transfer drops to 89%, and residual red Eu-centred emission can be easily detected. Further explorations of intermetallic f → d communications with other metallic pairs show that Cr^{III} can act as an acceptor in $[LnCr(\mathbf{L26})_3]^{6+}$ (Ln = Eu, $\eta_{Eu\rightarrow Cr}$ = 70%; Ln = Tb,

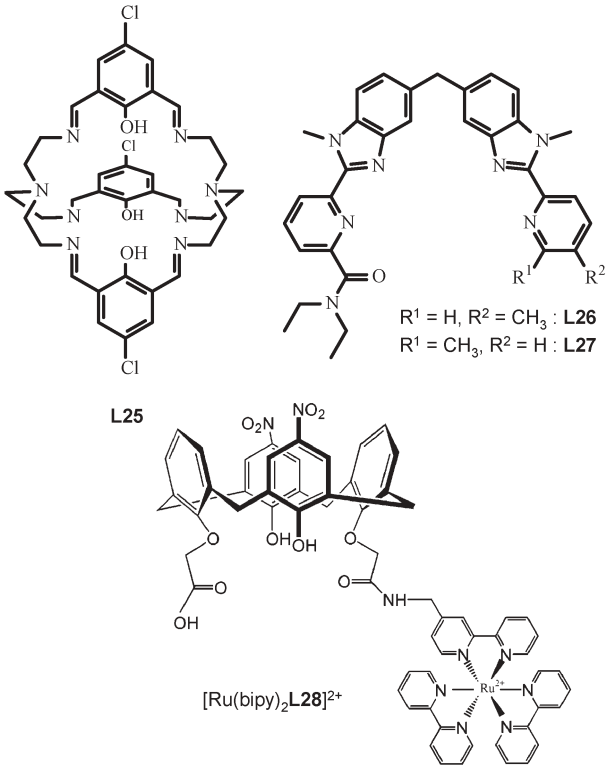

Scheme 9

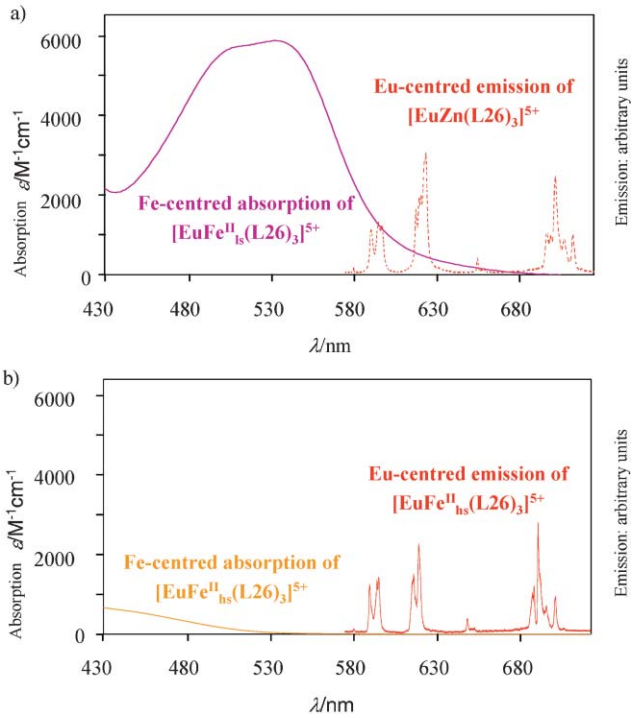

Fig. 14 Spectral overlap between the emission of the Eu^{III} donor and the absorption of the Fe^{II} acceptor in a) $[EuFe_{ls}(\mathbf{L26})_3]^{5+}$ and b) $[EuFe_{hs}(\mathbf{L27})_3]^{5+}$.[163,164]

$\eta_{Tb\rightarrow Cr}$ = 100%),[165] while quenching by Ru^{II} in $[Ru(bipy)_2(\mathbf{L28})Ln]^{5+}$ only occurs for Ln = Eu ($\eta_{Eu\rightarrow Ru}$ = 100%, while $\eta_{Tb\rightarrow Ru}$ = 0%).[166] Reverse d → f energy migration processes involving visible acceptor such as Eu^{III} or Tb^{III} are rare, owing to the high energies of the emitting $Eu(^5D_0)$ and $Tb(^5D_4)$ levels (Fig. 1).

The cyclometallated chromophore $[Ir^{III}C_2N_4]$ shown in Fig. 15 is a remarkable example, because it emits at a sufficiently high energy (21 740 cm^{-1}) to act as a donor for sensitizing Eu^{III} in the resulting heterotrimetallic complex with $\eta_{Ir\rightarrow Eu}$ = 38%.[167] Interestingly, the final Eu-centred red emission combines with the residual broad blue emission of the $[Ir^{III}C_2N_4]$ chromophore to give global white light emission. Obviously, the low-energy excited level of the NIR emitters Nd^{III}, Er^{III} and Yb^{III} are easier to be fed from a d-block donor, and d → f communications are common with Ru^{II},[90,166,168] Os^{II},[169] Re^{I},[169–172] Pt^{II},[172–175] and Cr^{III} donors.[40,90,176,177] The well-known kinetically inert low-spin d^6 chromophores $[Ru(bipy)_3]^{2+}$, $[Os(bipy)_3]^{2+}$ and $[Re(bipy)(CO)_3Cl]$ are shown to efficiently sensitize Ln = Nd, Er, Yb by using their ^{3}MLCT donor level (Schemes 8, 9, 10, Fig. 11), while square planar d^8 Pt^{II} complexes take advantage of their broad mixed ^{3}MLCT + ^{3}MMLCT emission levels (Fig. 16a). On the other hand, pseudo-octahedral Cr^{III} chromophores resort to spin-allowed ($Cr(^4T_1, {}^4T_2)$) and spin-forbidden ($Cr(^2E)$) excited states for sensitizing lanthanide NIR emitters (Fig. 16b).

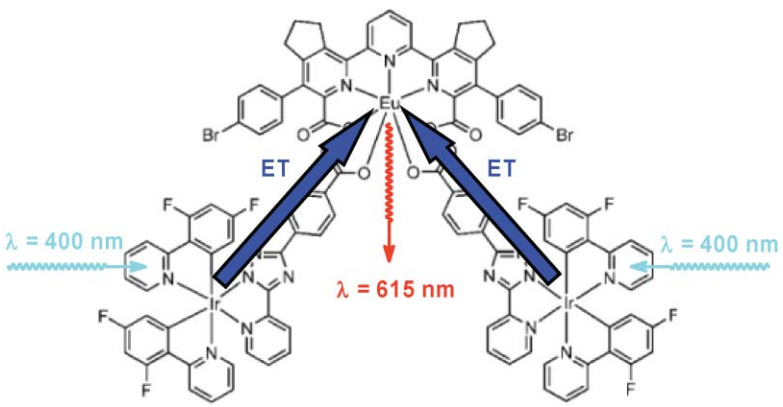

Fig. 15 Schematic representation of the intramolecular d → f energy transfer processes responsible for the sensitizing of Eu^{III} in a heterotrimetallic $[IrEuIr]^-$ assembly.[167]

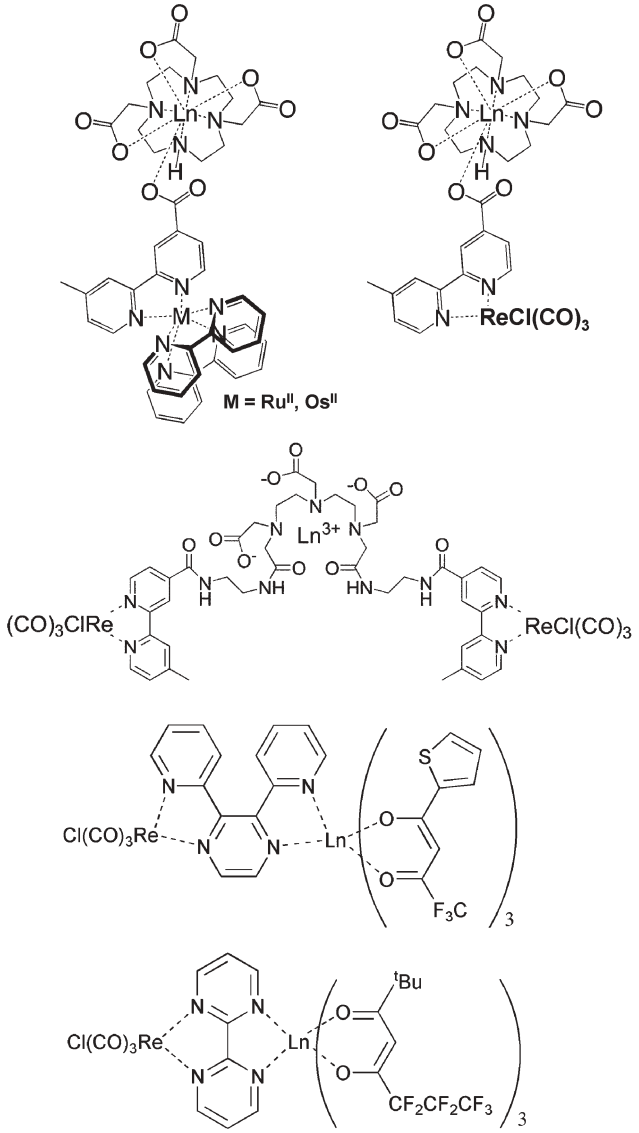

Scheme 10

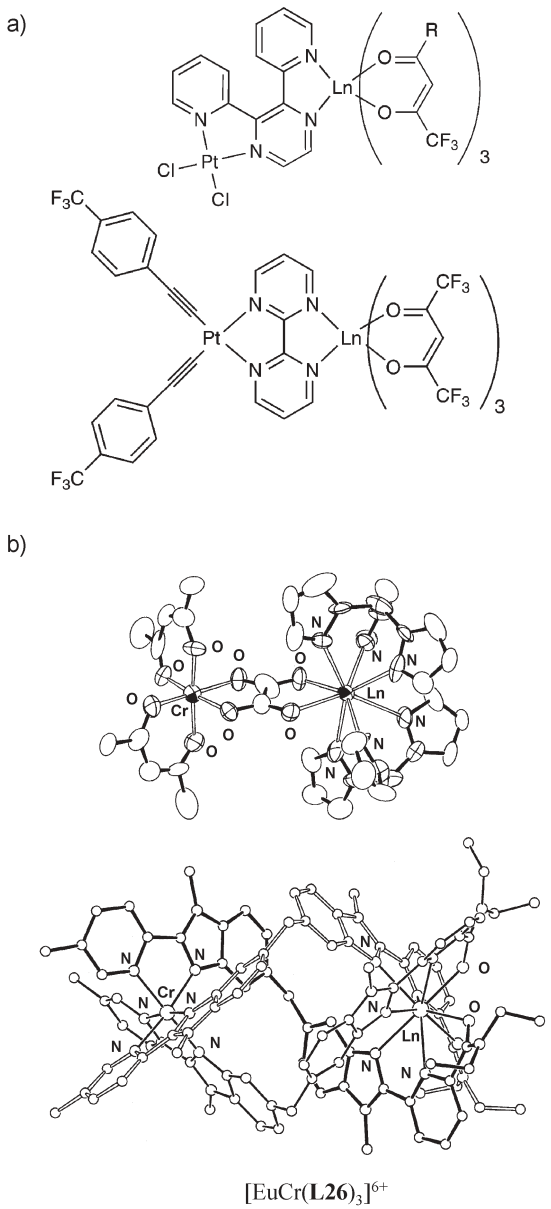

Fig. 16 Selected d–f complexes, in which a) low-spin d^8 and b) d^3 chromophores are used for sensitizing NIR luminescence (Ln = Nd, Er, Yb).[90,165,172,174,176,177]

4.1. Building the edifices

The absence of intermetallic scrambling processes is a prerequisite, when preparing discrete multimetallic complexes designed for the control of directional energy transfers. An obvious strategy relies on kinetic limitations associated with metal complexation to, and metal release from a receptor, as it has been successfully developed for main group chemistry (*i.e.* covalent synthesis). However, owing to the high lability of the ligands lying in the first coordination sphere of lanthanide metal ions,[178] this approach is rarely applicable. The alternative 'non-covalent' strategy aims at programming some thermodynamic selectivity between the complexation sites, which is eventually responsible for the recognition of the different metals in the final complexes. For heterobimetallic f–f complexes, the best reported thermodynamic discriminations[158,179] remain insufficient to quantitatively segregate between two lanthanide ions, and only mixtures are observed in dilute solutions compatible with luminescence measurements. Therefore, pure heterobimetallic f–f complexes are limited (i) to some solid state materials, which take advantage of kinetic resolution occurring during the crystallization process, and (ii) to the assembly of kinetically inert macrocyclic lanthanide complexes (porphyrin, phthalocyanin), as similarly reported by Faulkner and co-workers for $[Ln(DOTA)]^-$ building blocks (Fig. 12).[159,180,181] For d–f complexes, the use of kinetically inert pseudo-octahedral low-spin d^6 chromophores (Ru^{II}, Re^{I}, Os^{II}, Ir^{III}, Fig. 15 and Scheme 10), and pseudo-tetragonal d^8 Pt^{II} platforms (Fig. 16a) follows the same strategy, with the ultimate fixation of the labile f-block ion in the remaining empty coordination site. For inert d^3 Cr^{III}, Kaizaki and co-workers reacts the inert pre-organized pseudo-octahedral $[Cr(acac)_2(oxalate)]^-$

building block with Ln^{III} and tris(pyrazolylborate) (Tp^{-}) to give the heterobimetallic CrLn complexes shown in Fig. 16b (top).[177] A chiral version of the latter assembly is obtained when the racemic $[Cr(acac)_2(oxalate)]^{-}$ synthon is replaced with enantiomerically pure Λ-$[Cr(acac)_2(oxalate)]^{-}$. A high degree of diastereoselectivity is observed leading to the exclusive formation of {Λ-$[Cr(acac)_2(oxalate)]$-Δ-$[Ln(Tp)_2]$}.[176,182,183] A completely different strategy has been developed for the preparation of the triple-stranded helicates $[CrLn(\mathbf{L26})_3]^{6+}$ (Fig. 16b, bottom).[165] The assembly of the bimetallic helix is performed around the kinetically labile pair Cr^{II}–Ln^{III} to provide the air-sensitive complex $[Cr^{II}Ln(\mathbf{L26})_3]^{5+}$, which is then easily oxidized to give $[Cr^{III}Ln(\mathbf{L26})_3]^{6+}$. Interestingly, the subsequent de-complexation of Ln^{III} produces an inert racemic C_3-symmetrical tripod *rac*-$[Cr(\mathbf{L26})_3]^{3+}$, which can be separated into its helical enantiomers (Fig. 17).[184] The subsequent recombination of each enantiomer with Ln^{III} eventually leads to the enantiomerically pure triple helices *PP*-$[CrLn(\mathbf{L26})_3]^{6+}$ and *MM*-$[CrLn(\mathbf{L26})_3]^{6+}$, whose specific optical properties have been exploited (see section 4.3).

4.2. Extending the lifetime of excited levels

When one metal ion is used as a donor for sensitizing the emission of a second accepting metal ion, the characteristic lifetimes τ of their excited states, which are related to their deactivation rates by $\tau = k^{-1}$, are affected by the intermetallic communication process. This situation can be simply modelled for the special case of a d–f pair, in which the d-block chromophore (M) sensitizes the neighbouring lanthanide ion

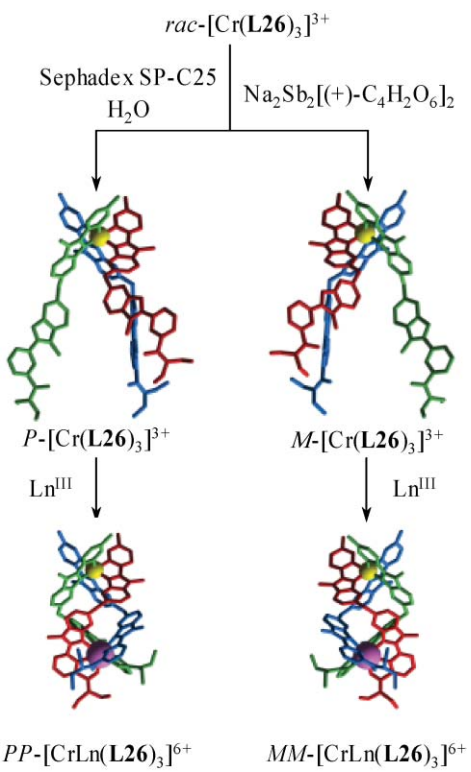

Fig. 17 Chiral resolution of the tripodal complex *rac*-$[Cr(\mathbf{L26})_3]^{3+}$and synthesis of the enantiomerically pure triple helices *PP*-$[CrLn(\mathbf{L26})_3]^{6+}$ and *MM*-$[CrLn(\mathbf{L26})_3]^{6+}$.[184]

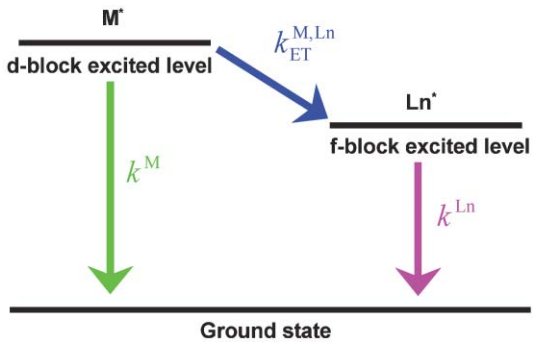

Fig. 18 Kinetic model for the deactivation processes and communication between d-block and f-block-centred excited levels in $[MLn(\mathbf{L26})]^{5/6+}$ (M = Cr, Ru; Ln = Nd, Er, Yb).[90] Adapted from ref. 90.

(Ln) thanks to an energy transfer process $k_{ET}^{M,Ln}$ (Fig. 18). In the absence of energy transfer, both the excited states of the isolated chromophore possess their intrinsic deactivation rates k^{M} and k^{Ln}, respectively, which provides the standard rate equations (8) and (9).

$$d[M^*(t)]/dt = -(k_{ET}^{M,Ln} + k^{M})\cdot[M^*(t)] \quad (8)$$

$$d[Ln^*(t)]/dt = k_{ET}^{M,Ln}\cdot[M^*(t)] - k^{Ln}[Ln^*(t)] \quad (9)$$

Integration gives equations (10) and (11), which are required for correctly interpreting the effect of intermetallic communication on the luminescence in a metallic pair.

$$[M^*(t)] = [M^*(0)]\cdot e^{-(k_{ET}^{M,Ln}+k^{M})\cdot t} \quad (10)$$

$$[Ln^*(t)] = [M^*(0)]\cdot\frac{k_{ET}^{M,Ln}}{k^{Ln}-(k_{ET}^{M,Ln}+k^{M})}\cdot\left(e^{-(k_{ET}^{M,Ln}+k^{M})\cdot t} - e^{-k^{Ln}\cdot t}\right) \quad (11)$$

Eqn (10) reveals that the decay rate of the excited state of the donor [M^*] (*i.e.* the d-block ion in our example) is increased, when an energy transfer occurs toward an acceptor. The experimental decay of the d-block ion thus corresponds to the sum of the two deactivation rate constants $k_{obs}^{M} = k^{M} + k_{ET}^{M,Ln}$, which translates into a reduced lifetime $\tau^{M} = (k_{obs}^{M})^{-1} = (k^{M} + k_{ET}^{M,Ln})^{-1}$. Interpretation of eqn (11) is trickier, because the magnitude of $k_{ET}^{M,Ln}$ controls the feeding rate of the excited state of the acceptor (*i.e.* the f-block ion in our example). Therefore, the profile of [$Ln^*(t)$] after the initial excitation of the donor d-block metal strongly depends on the relative magnitudes of the rate constants $k_{obs}^{M} = k^{M} + k_{ET}^{M,Ln}$ and k^{Ln}.[90] The first limiting case considers $k_{obs}^{M} \gg k^{Ln}$, for which the Ln^* level is almost completely fed before any significant Ln-centred deactivation occurs. We can thus easily predict that the experimental Ln-centred deactivation rate k_{exp}^{Ln} mirrors that found in absence of intermetallic communication k^{Ln}. Introducing the specific condition $k_{obs}^{M} \gg k^{Ln}$ in eqn (11) produces eqn (12), whereby the time dependence of the decay profile indeed corresponds to $k_{exp}^{Ln} = k^{Ln}$.

$$[Ln^*(t)] = [M^*(0)]\cdot\frac{k_{ET}^{M,Ln}}{k_{ET}^{M,Ln}+k^{M}}\cdot e^{-k^{Ln}\cdot t} \quad (12)$$

This situation is encountered for a large number of d–f pairs, because the intrinsic deactivation rates of the d-block donors k^{M} are often considerably larger than the deactivation of the Ln-centred 4f excited states (Laporte-forbidden transitions). For instance, it occurs for the Ru → Yb communication in $[RuYb(\mathbf{L26})_3]^{5+}$ (Fig. 19a). As expected, the experimental decay rate of the donor $k_{obs}^{Ru} = 1.2 \times 10^5\ s^{-1}$ is increased with respect to $k^{Ru} = 1.0 \times 10^5\ s^{-1}$ (measured for $[RuGd(\mathbf{L26})_3]^{5+}$ in the absence of an intermetallic energy transfer process), which is diagnostic for the existence of the Ru → Yb energy transfer. Since $k_{obs}^{Ru} = 1.2 \times 10^5\ s^{-1} > k^{Yb} = 5 \times 10^4\ s^{-1}$ (measured for $[ZnYb(\mathbf{L26})_3]^{5+}$ in the absence of intermetallic energy transfer), eqn (12) predicts that the experimental Yb-centred decay rate recorded in $[RuYb(\mathbf{L26})_3]^{5+}$ should roughly mirror k^{Yb}, and this is indeed observed with an experimental value of $k_{exp}^{Yb} = 4.4 \times 10^4\ s^{-1}$ (Fig. 19a).[90] The second limiting case arises when $k_{obs}^{M} \ll k^{Ln}$, in other words when the Ln-centred excited state Ln^* almost instantaneously relaxes as long as it is slowly fed by the donor d-block chromophore. We logically conclude, that the deactivation of the d-block ion ($k_{obs}^{M} = k^{M} + k_{ET}^{M,Ln}$) controls the overall deactivation process, and the experimental Ln-centred deactivation rate k_{exp}^{Ln} would mirror k_{obs}^{M}. Again, the introduction of the condition $k_{obs}^{M} \ll k^{Ln}$ into eqn (11), provides a simplified eqn (13), which demonstrates that the time dependence of the decay profile indeed corresponds to $k_{exp}^{Ln} = k_{obs}^{M}$.

$$[Ln^*(t)] = [M^*(0)]\cdot\frac{k_{ET}^{M,Ln}}{k^{Ln}}\cdot e^{-\left(k_{ET}^{M,Ln}+k^{M}\right)\cdot t} = [M^*(0)]\cdot\frac{k_{ET}^{M,Ln}}{k^{Ln}}\cdot e^{-k_{obs}^{M}\cdot t} \quad (13)$$

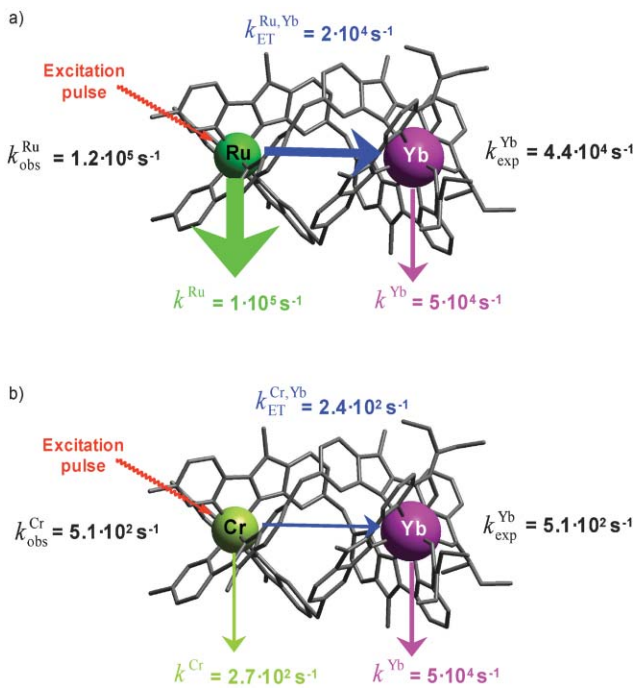

Fig. 19 Interpretation of the rate equations (10)–(13). Illustrations of a) the first limiting case $k_{obs}^{M} >> k^{Ln}$, observed in $[RuYb(\mathbf{L26})_3]^{5+}$, and b) the second limiting case $k_{obs}^{M} \ll k^{Ln}$, observed in $[CrYb(\mathbf{L26})_3]^{6+}$.[90]

The replacement of Ru^{II} with Cr^{III} as the donor in $[CrYb(\mathbf{L26})_3]^{6+}$ illustrates this second situation because the combination of the intrinsic deactivation of the Cr-centred donor levels $k^{Cr} = 2.7 \times 10^2\ s^{-1}$ (measured in $[CrGd(\mathbf{L26})_3]^{6+}$), with the rate of energy transfer $k_{ET}^{Cr,Yb} = 2.4 \times 10^2\ s^{-1}$ gives $k_{obs}^{Cr} = k^{Cr} + k_{ET}^{Cr,Yb} = 5.1 \times 10^2\ s^{-1}$, which remains small compared to the intrinsic rate of deactivation of $Yb(^2F_{5/2})$ ($k^{Yb} = 5 \times 10^4\ s^{-1}$ measured in $[ZnYb(\mathbf{L26})_3]^{5+}$, and $k^{Yb} >> k_{obs}^{M}$, Fig. 19b).[90] As expected (eqn 13), the experimental decay of the Yb-centred emission amounts to $k_{exp}^{Yb} = 5.1 \times 10^2\ s^{-1}$, which perfectly mirrors the slow deactivation of the Cr^{III} chromophore k_{obs}^{Cr}. These rate constants can be transformed into characteristic excited lifetimes, thus leading to $\tau_{exp}^{Yb} = (k_{exp}^{Yb})^{-1} = 23\ \mu s$, when Yb^{III} is sensitized by Ru^{II} in $[RuYb(\mathbf{L26})_3]^{5+}$, and $\tau_{exp}^{Yb} = (k_{exp}^{Yb})^{-1} = 1960\ \mu s = 1.96\ ms$, when Yb^{III} is sensitized by Cr^{III} in the isostructural complex $[CrYb(\mathbf{L26})_3]^{6+}$.[90] Such apparent extension of the Ln-centred NIR luminescence lifetime by two or three orders of magnitude (from the microsecond to the millisecond range) may be valuable for improving the sensitivity of time-gated homogeneous fluoroimmunoassays, assuming a judicious choice of the donor chromophore (see section 2.3 and Fig. 4c).

4.3. Chiral luminescent probes

When lanthanide complexes lack of symmetry elements of the second kind, chirality results as with any other molecules, and specific interactions with electromagnetic waves can be detected.[185,186] Three types of circular dichroism (CD) methods are employed in chirality sensing involving lanthanide complexes:[187] (1) Ln-centred CD absorption spectra based on intraconfigurational f–f transitions,[182,183] (2) CD absorption spectra of the coordinated chromophoric ligands,[188,189] and (3) Ln-centred circularly polarized luminescence (CPL), which is the emissive pending of metal-centred CD absorption spectra mentioned above.[190] The two Ln-centred methods differ from one another in two main ways. Firstly, due to the Franck–Condon principle, CPL probes the chiral geometry of the excited states in the same way that CD probes the ground state structures. Secondly, CPL measurements also reflect molecular motions and energetics that take place between the excitation (absorption) and emission. This close relationship is further evidenced by the spectroscopic characteristics since CD measures the difference in absorption between left (molar absorption coefficient ε_L) and right (ε_R) circularly polarized light (eqn 14), while CPL measures the difference in emission intensity between left (I_L) and right (I_R) circularly polarized light (eqn 15).[190]

$$g_{abs} = \frac{\Delta\varepsilon}{1/2(\varepsilon)} = \frac{\varepsilon_L - \varepsilon_R}{1/2(\varepsilon_L + \varepsilon_R)} \quad (14)$$

$$g_{lum} = \frac{\Delta I}{1/2(I)} = \frac{I_L - I_R}{1/2(I_L + I_R)} \quad (15)$$

Since this review is focused on luminescence, only CPL measurements will be further discussed. The luminescence dissymmetry factors g_{lum} can be correlated to molecular parameters thanks to eqn (16) (assuming the isotropic limit),

whereby $f_{CPL}(\lambda)$ and $f_{TL}(\lambda)$ are specific line-shape functions for circularly polarized luminescence and total luminescence, and μ^{gn} and m^{gn} refer to the electric dipole and magnetic dipole transitions.[190]

$$g_{lum}(\lambda) = 4\frac{f_{CPL}(\lambda)}{f_{TL}(\lambda)}\left[\frac{\mu^{gn}\cdot m^{gn}}{|\mu^{gn}|^2}\right] \quad (16)$$

Eqn (16) indeed illustrates the operational principle of CPL spectroscopy. Since the denominator becomes very large for dipole-allowed transitions, CPL focuses on formally Laporte-forbidden transitions. Moreover, the numerator is concomitantly proportional to the magnetic dipole transition, which becomes significant when helical charge displacement occurs. These two requirements are met for the Laporte-forbidden, but magnetic dipole-allowed Eu($^5D_0 \rightarrow {}^7F_1$), Tb($^5D_4 \rightarrow {}^7F_5$) and Yb($^2F_{5/2} \rightarrow {}^2F_{7/2}$) transitions, when the metal is coordinated to three[191] or four[192] helically wrapped ligand strands forming enantiomerically pure pseudo-C_3 and pseudo-C_4-symmetrical complexes. The most common synthetic strategy relies on the use of enantiomerically pure organic receptor possessing several kinetically inert stereogenic carbon centres, which are able to react with Ln^{III} with a high degree of diastereoselectivity to give a single helical (*P* or *M*) isomer in solution. Scheme 11 collects some chiral linear (**L29–L31**),[193–195] tripodal (**L32–L33**),[196–197] and tetrapodal (**L34–L38**) receptors[198–205] commonly used for preparing optically active complexes with luminescent lanthanides (Ln = Nd, Eu, Tb, Yb). For the linear ligands, both **L29**[193] and **L30**[194] give

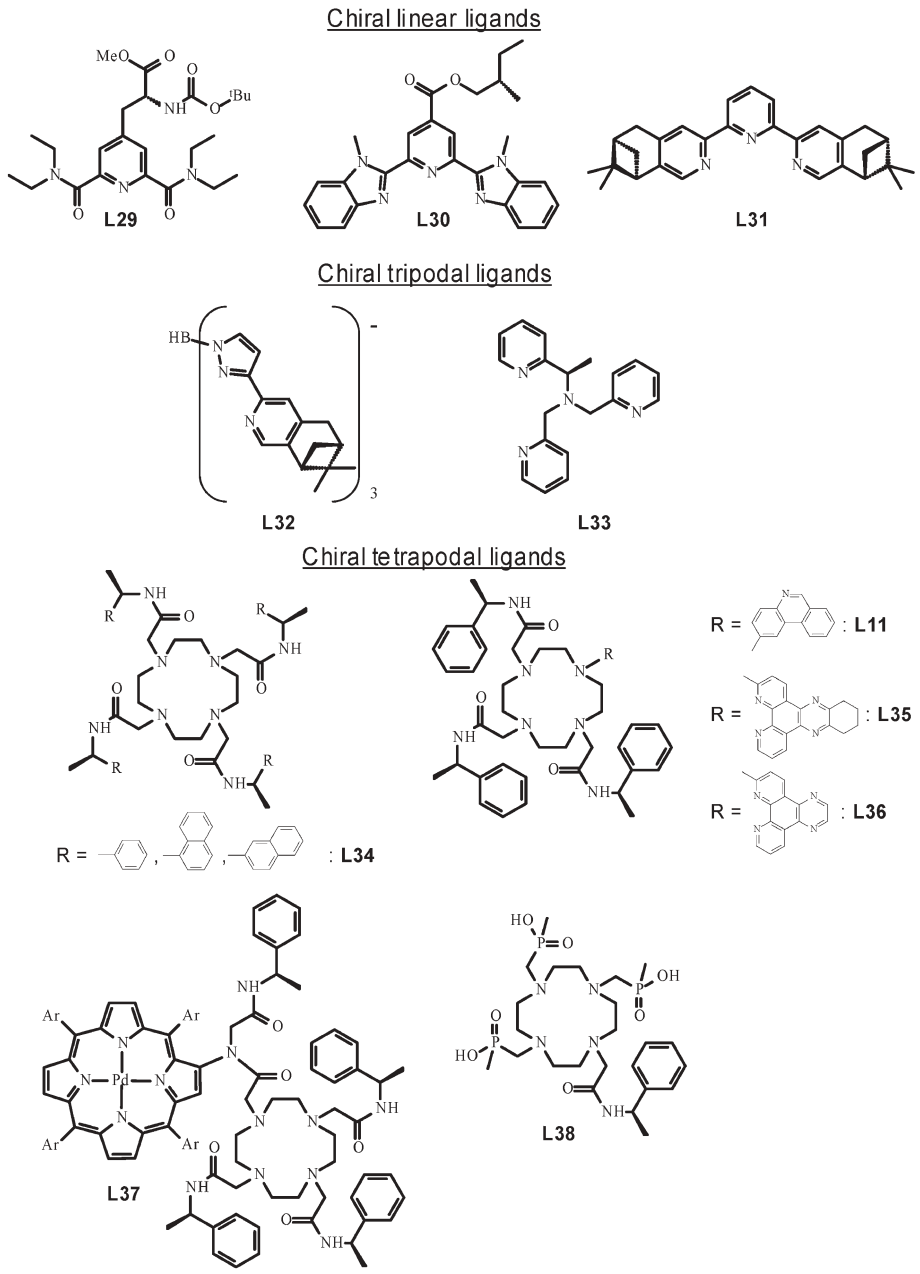

Scheme 11

mixtures of labile $[Ln(\mathbf{Li})_2]^{3+}$ and $[Ln(\mathbf{Li})_3]^{3+}$ complexes (Ln = Eu, Tb) with only very limited diastereomeric excesses, but **L31** produces a single helical diastereomer $[Eu(\mathbf{L31})_3]^{3+}$ characterized by a moderate dissymmetry factor $g_{lum}(^5D_0 \rightarrow {}^7F_1) = 0.020$.[195] Unfortunately, no CPL measurements have been reported for the chiral complexes $[Tb(\mathbf{L32})(NO_3)_2]$[196] and $[Ln(\mathbf{L33})_n]^{3+}$,[197] which could have brought some clue on the chiral induction associated with pseudo-C_3-symmetrical receptors. Conversely, the CPL spectra of the pseudo-C_4-symmetrical complexes based on the macrocyclic cyclen platforms **L34–L38** have been extensively investigated in the visible (Ln = Eu, Tb) and in the NIR (Ln = Nd, Yb) spectral domains.[198–205] Large dissymmetry factors have been reported for $Tb(^5D_4 \rightarrow {}^7F_5)$ in $[Tb(\mathbf{L34})]^{3+}$ ($g_{lum} = 0.17$)[198] and $[Tb(\mathbf{L38})]^{3+}$ ($g_{lum} = 0.17$),[205] and for $Eu(^5D_0 \rightarrow {}^7F_1)$ in $[Eu(\mathbf{L34})]^{3+}$ ($g_{lum} = 0.18$),[198] Interestingly, comparable g_{lum} are found in the NIR for $Yb(^2F_{5/2} \rightarrow {}^2F_{7/2})$ in $[Yb(\mathbf{L11})]^{3+}$ ($g_{lum} \geqslant 0.1$),[200] while the very weak value $g_{lum} = 0.0015$ observed for the emission of the magnetic-forbidden transition $Nd(^4F_{3/2} \rightarrow {}^4F_{9/2})$ in $[Nd(\mathbf{L37})]^{3+}$ may be easily rationalized with eqn (16).[204] The obvious application of these chiral complexes concerns their use as luminescent probes for sensing chiral (biological) substrates, whose specific interactions with the Ln centres induce noticeable changes in the CD and/or CPL responses.[199] Taking advantage of the peripheral planar aromatic porphyrin metallamacrocycle in $[Ln\mathbf{L37}]^{3+}$,[204] or of the tetra-azatriphenylene rings in $[Ln\mathbf{L35}]^{3+}$ and $[Ln\mathbf{L36}]^{3+}$, selective intercalation in DNA has been demonstrated,[201,204] together with *in cellulo* imaging potentials.[202,203] For racemic lanthanide complexes, the interaction with a chiral substrate may stabilize one particular diastereomer, thus producing a diastereomeric excess coupled with CD and CPL signals (*i.e.* the Pfeiffer effect).[187,189,191,192] For instance, the simple triple helical C_3-symmetrical $[Pr(2,2'\text{-oxydiacetate})_3]^{3-}$ interacts with L-proline in its ground state to generate a significant residual CD spectrum.[206] Such interactions can be monitored in the excited states by using CPL, and the enantioselective quenching of the closely related C_3-symmetrical [Ln(2,6-pyridinedicarboxylate)]$^{3-}$ with biomolecules,[191] or with resolved octahedral d-block complexes[207] have been intensively explored. Except for the use of the Pd-porphyrin complex as sensitizer in the chiral complex $[Yb\mathbf{L37}]^{3+}$,[204] the measurement of CPL in multimetallic d–f or f–f discrete heteropairs is restricted to the recent resolution of $[EuCr(\mathbf{L26})_3]^{6+}$ into its *PP* and *MM* helical enantiomers (Fig. 17).[184] The CD spectra show opposite Cotton effects, whose energy sequence can be rationalized by the simultaneous modelling of intra- and internuclear exciton couplings involved in the $([Eu(\text{benzimidazole-pyridine})_3]^{3+}$ and $[Cr(\text{benzimidazole-pyridine})_3]^{3+}$ chromophores.[188] The associated metal-centred CPL signals confirm the existence of pure helical enantiomers displaying dual $Eu(^5D_0)$ and $Cr(^2E)$ luminescence with $g_{lum}^{Eu} = \pm 0.16$ ($^5D_0 \rightarrow {}^7F_1$) and $g_{lum}^{Cr} = \pm 0.01$ ($^2E \rightarrow {}^4A_2$, Fig. 20).[184] Due to the quantitative intramolecular Tb → Cr energy transfer occurring in $[TbCr(\mathbf{L26})_3]^{6+}$, the polarized emission of the associated pure enantiomers *PP*-$[TbCr(\mathbf{L26})_3]^{6+}$ and *MM*-$[TbCr(\mathbf{L26})_3]^{6+}$ shows exclusively the Cr-centred luminescence. These data suggest that C_3 and particularly C_4-symmetrical helicity is an efficient tool for inducing large CPL signals, which can be further modulated by enantioselective interactions with chiral substrates.

5. Shaping the future

General trends

The variety of applications reviewed above reflects the rich spectroscopy of the trivalent lanthanide ions, some of them featuring more than a thousand electronic levels. It is quite obvious that well-established applications in optics (lasers, optical fibres) and lighting will continue to make use of lanthanide-containing materials. Moreover, the synergy

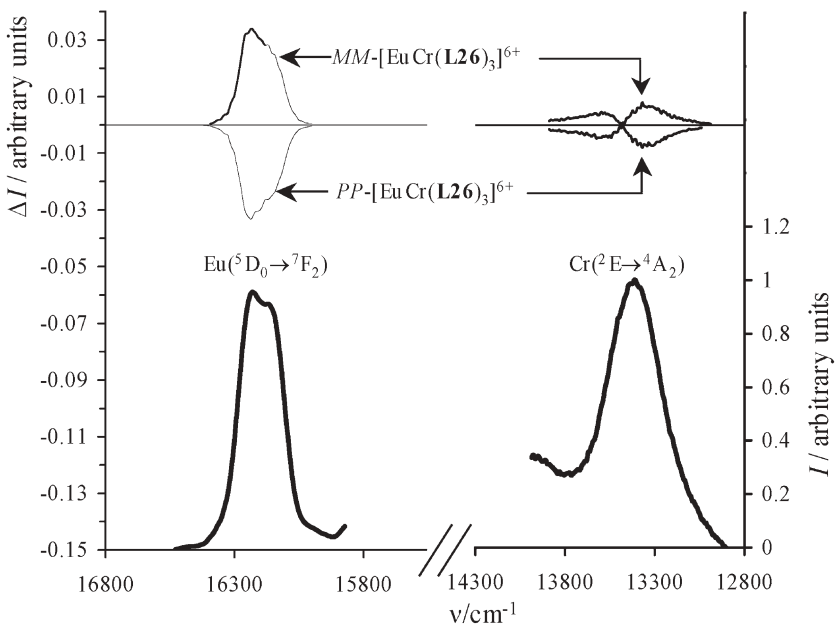

Fig. 20 Circularly polarized luminescence (CPL) of $[EuCr(\mathbf{L26})_3]^{6+}$ in acetonitrile (adapted from ref. 184).

between coordination chemistry and photochemistry which emerged about thirty years ago has produced numerous responsive lanthanide-containing complexes, based on very diverse chelating agents. These complexes allow the monitoring of a range of analytes, from simple anions or cations to elaborate biological substrates through time-resolved luminescent immunoassays. For instance, DNA and mRNA can be detected without the use of polymerase chain reactions (PCR) to amplify the amount of samples. In our opinion, attention in the near future will be focused on several facets of lanthanide luminescence, given the fact that synthetic methods for the design of adequate Ln^{III} receptors are essentially at hand and do not constitute a handicap anymore.

Firstly, since a number of recently proposed luminescent labels proved to be suitable for imaging purposes, and since there is a heavy need for targeted diagnostic imaging and for the follow up of reactions taking place in living cells, going not only "*in vivo*", but also and mainly "*in cellulo*" will constitute the key challenge for future lanthanide-based luminescent responsive systems. A combination of polymer techniques, such as those presently developed for organic light emitting diodes,[11] and biochemical reactions may lead to new classes of efficient luminescent sensors. Indeed, self-quenching of lanthanide ions is very small owing to the very low oscillator strengths of the 4f–4f transitions and high concentrations of ions can be inserted into polymers, leading to highly luminescent stains. Similarly, nanoparticle labels are now attracting interest for the same reason.[208] Secondly, we anticipate progress in chirality probes, the potential of which has not yet been fully exploited, maybe because the relationship between CPL effects and the structure of the chiral edifices generating them is not fully understood. Thirdly, efforts are starting to emerge to improve several technical aspects, including instrumentation and excitation mode. With respect to the latter, two-photon absorption is probably a valid option and a recent work demonstrates efficient excitation of a neutral ternary complex $[Eu(tta)_3(dpbt)]$ (dpbt stands for 2-(*N*,*N*-diethylaniline-4-yl)-4,6-bis(3,5-dimethylpyrazol-1-yl)-1,3,5-triazine) in the range 745–800 nm. The *N*,*N*-diethylaniline moiety of the dpbt chromophore is an electron donor, while the dipyrazoyltriazine group acts as the electron acceptor, and donor–acceptor character is indeed the structural basis for efficient two-photon absorption.[209] Considering the advantages linked with the use of NIR emitting luminescent probes, one may predict that an ideal luminescent diagnostic assay could feature such a probe with an excitation at 980 nm, a wavelength for which cheap laser diodes are available.

Multimetallic edifices: control of luminescent properties and/or sensitization

According to the considerable perspectives offered by intermetallic communications involving a f-block metal ion, and to their simple modelling with the rate equations (8)–(11), the ultrafine tuning of energy transfers leading to delayed Ln-centred luminescence is within reach. Until now, attention has been mainly focused on the charge transfer transitions occurring with low-spin d^6 and d^8 metal ions, but a plethora of d–d transitions are accessible for further extensions. Although characterized by very weak oscillator strengths, spin-forbidden d–d excited states can play a crucial role as relays in energy migration processes, because their intrinsic long lifetimes significantly increase the eventual Ln-centred emission, as demonstrated in $[CrYb(\mathbf{L26})_3]^{6+}$ (Fig. 19). When the tuning of the energy levels is foreseen, the poor mixing of the electronic and vibrational wave functions in 4f-centred excited states appears as a considerable advantage, and intermetallic f–f communication should greatly improve our capacity to rationally manipulate energy funnelling in discrete molecules. However, the lack of suitable thermodynamic selectivity for introducing different lanthanides in the same architecture remains deleterious for the development of this topic. The use of kinetically inert porphyrin, phthalocyanin or cyclen macrocyclic complexes remains too limited to offer a

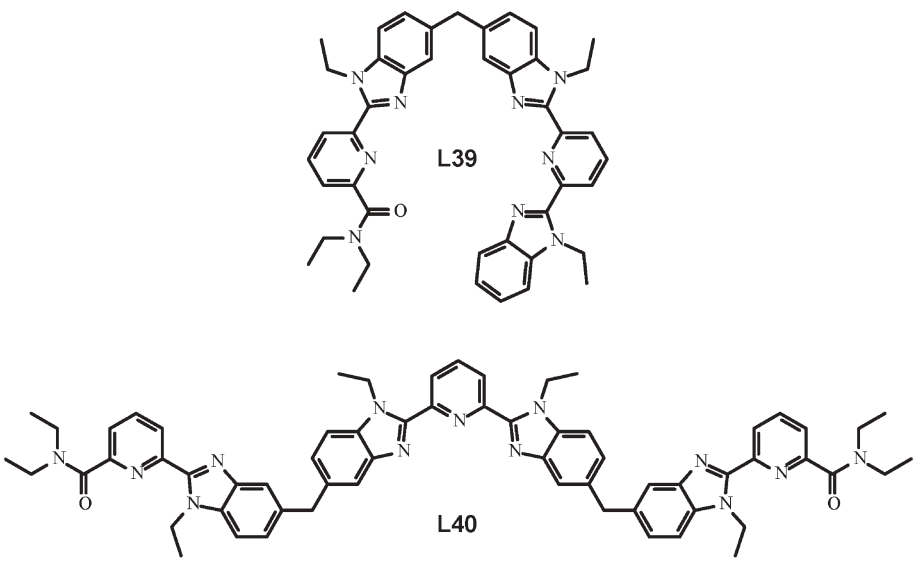

Scheme 12

valuable alternative to thermodynamic control, and the programming of intermetallic repulsion and interligand interactions in multicomponent assemblies is becoming an unavoidable chemical challenge for preparing pure heteropolymetallic f–f systems. The recent (more or less) planned rational deviations from statistics observed in solution for the bimetallic $[LaLu(\mathbf{L39})_3]^{6+}$[179] and the trimetallic $[EuLaEu(\mathbf{L40})_3]^{9+}$ helicates[210] (Scheme 12) suggest that a predictable access to local dielectric constants may contribute to address this challenge.

Acknowledgements

The authors thank the collaborators of their research groups for their important experimental input and the Swiss National Science Foundation for financial support.

References

1 E. N. Harvey, *A History of Luminescence. From the Earliest Times Until 1900*, American Philosophical Society, Philadelphia, 1957.
2 W. H. Melhuish, *Pure Appl. Chem.*, 1984, **56**, 231.
3 N. Kaltsoyannis and P. Scott, *The f elements*, Oxford Chemistry Primers, ed. J. Evans, Oxford Science Publications, Oxford, 1999.
4 S. Cotton, *Lanthanides and actinides*, McMillan Physical Science Series, McMillan Education, London, 1991.
5 W. Crookes, *Philos. Trans. R. Soc. London, Ser. A*, 1885, **176**, 691.
6 G. Urbain, *Ann. Chim. Phys., Ser. 8*, 1909, **18**, 222.
7 L. Ozawa and M. Itoh, *Chem. Rev.*, 2003, **103**, 3835.
8 T. Kojima, in *Phosphor Handbook*, eds. S. Shionoya and W. M. Yen, CRC Press, Boca Raton, 1999, Ch. 10, 623–36.
9 J.-C. G. Bünzli, in *Spectroscopic Properties of Rare Earths in Optical Materials*, eds. G. K. Liu and B. Jacquier, Springer Verlag, Berlin, 2005, Vol. 83, Ch. 11.
10 S. Shionoya and W. M. Yen, *Phosphor Handbook*, CRC Press Inc., Boca Raton, FL, 33431, USA, 1999.
11 J. Kido and Y. Okamoto, *Chem. Rev.*, 2002, **102**, 2357.
12 K. Matsumoto and J. G. Yuan, *Lanthanide Chelates as Fluorescent Labels for Diagnostics and Biotechnology*, Metal Ions in Biological Systems, eds. A. Sigel and H. Sigel, Vol. 40, Ch. 6, Marcel Dekker Inc., New York, 2003.
13 (*a*) S. Faulkner and J. L. Matthews, in *Comprehense Coordination Chemistry II*, ed. M. D. Ward, Elsevier Pergamon, Amsterdam, 2004, Vol. 9, Ch. 9.21, 913–44; (*b*) V. W. W. Yam and K. K. W. Lo, *Coord. Chem. Rev.*, 1999, **184**, 157.
14 S. Faulkner, S. J. A. Pope and B. P. Burton-Pye, *Appl. Spectrosc. Rev.*, 2005, **40**, 1.
15 W. T. Carnall, P. R. Fields and K. Rajnak, *J. Chem. Phys.*, 1968, **49**, 4450.
16 M. H. V. Werts, R. T. F. Jukes and J. W. Verhoeven, *Physical Chemistry Chemical Physics*, 2002, **4**, 1542.
17 W. T. Carnall, *The Absorption and Fluorescence Spectra of Rare Earth Ions in Solution*, Handbook on the Physics and Chemistry of Rare Earths, ed. K. A. Gschneidner, Jr. and L. Eyring, Vol. 3, Ch. 24, North Holland Publ. Co., Amsterdam, 1979.
18 W. T. Carnall, P. R. Fields and K. Rajnak, *J. Chem. Phys.*, 1968, **49**, 4424.
19 W. T. Carnall, P. R. Fields and K. Rajnak, *J. Chem. Phys.*, 1968, **49**, 4447.
20 W. T. Carnall, P. R. Fields and K. Rajnak, *J. Chem. Phys.*, 1968, **49**, 4443.
21 R. T. Wegh, H. Donker, K. D. Oskam and A. Meijerink, *Science*, 1999, **283**, 663.
22 I. Hemmilä and V. M. Mukkala, *Crit. Rev. Clin. Lab. Sci.*, 2001, **38**, 441.
23 I. Hemmilä, T. Ståhlberg and P. Mottram, *Bioanalytical Applications of Labelling Technologies*, Wallac Oy, Turku, 1995.
24 A. I. Voloshin, N. M. Shavaleev and V. P. Kazakov, *J. Lumin.*, 2001, **93**, 199.
25 F. Auzel, *Chem. Rev.*, 2004, **104**, 139.
26 J. W. Stouwdam, G. A. Hebbink, J. Huskens and F. C. J. M. Van Veggel, *Chem. Mater.*, 2003, **15**, 4604.
27 M. Latva, H. Takalo, V. M. Mukkala, C. Matachescu, J.-C. Rodriguez-Ubis and J. Kankare, *J. Lumin.*, 1997, **75**, 149.
28 R. D. Archer, H. Y. Chen and L. C. Thompson, *Inorg. Chem.*, 1998, **37**, 2089.
29 F. Gutierrez, C. Tedeschi, L. Maron, J. P. Daudey, R. Poteau, J. Azema, P. Tisnes and C. Picard, *Dalton Trans.*, 2004, 1334.
30 G. F. de Sá, O. L. Malta, C. D. Donega, A. M. Simas, R. L. Longo, P. A. Santa-Cruz and E. F. da Silva, *Coord. Chem. Rev.*, 2000, **196**, 165.
31 F. R. Gonçalves e Silva, O. L. Malta, C. Reinhard, H. U. Güdel, C. Piguet, J. E. Moser and J.-C. G. Bünzli, *J. Phys. Chem. A*, 2002, **106**, 1670.
32 F. R. Gonçalves e Silva, R. L. Longo, O. L. Malta, C. Piguet and J.-C. G. Bünzli, *Phys. Chem. Chem. Phys.*, 2000, **2**, 5400.
33 J.-C. G. Bünzli and C. Piguet, in *Encyclopedia of Materials: Science and Technology*, eds. K. H. J. Buschow, R. W. Cahn, M. C. Flemings, B. Ilschner, E. J. Kramer and S. Mahajan, Elsevier Science Ltd, Oxford, 2001, Vol. 10, Ch. 1.10.4, 4465–76.
34 J.-C. G. Bünzli, in *Metal Complexes in Tumor Diagnosis and as Anticancer Agents*, eds. A. Sigel and H. Sigel, Marcel Dekker Inc., New York, 2004, Vol. 42, Ch. 2, 39–75.
35 G. Blasse, *Chemistry and Physics of Rare-Earth Activated Phosphors*, Handbook on the Physics and Chemistry of Rare Earths, eds. K. A. Gschneidner, Jr. and L. Eyring, Vol. 4, Ch. 34, North Holland Publ. Co., Amsterdam, 1979.
36 S. Petoud, J.-C. G. Bünzli, T. Glanzman, C. Piguet, Q. Xiang and R. P. Thummel, *J. Lumin.*, 1999, **82**, 69.
37 T. Justel, H. Nikol and C. Ronda, *Angew. Chem. Int. Ed.*, 1998, **37**, 3085.
38 M. D. Seltzer, *J. Chem. Educ.*, 1995, **72**, 886.
39 N. M. Shavaleev, G. Accorsi, D. Virgili, Z. R. Bell, T. Lazarides, G. Calogero, N. Armaroli and M. D. Ward, *Inorg. Chem.*, 2004, **44**, 61.
40 D. Imbert, M. Cantuel, J.-C. G. Bünzli, G. Bernardinelli and C. Piguet, *J. Am. Chem. Soc.*, 2003, **125**, 15698.
41 A. P. De Silva, D. B. Fox, A. J. M. Huxley and T. S. Moody, *Coord. Chem. Rev.*, 2000, **205**, 41.
42 S. Hüfner, *Optical Spectra of Transparent Rare Earth Compounds*, Academic Press, New York, 1978.
43 A. Beeby, I. M. Clarkson, R. S. Dickins, S. Faulkner, D. Parker, L. Royle, A. S. de Sousa, J. A. G. Williams and M. Woods, *J. Chem. Soc., Perkin Trans. 2*, 1999, 493.
44 R. M. Supkowski and W. D. Horrocks, Jr., *Inorg. Chim. Acta*, 2002, **340**, 44.
45 J.-C. G. Bünzli, in *Rare Earths*, eds. R. Saez Puche and P. Caro, Editorial Complutense, Madrid, 1998, 223–59.
46 R. M. Izatt, K. Pawlack, J. S. Bradshaw and R. L. Bruening, *Chem. Rev.*, 1991, **91**, 1721.
47 G. R. Choppin, in *Lanthanide Probes in Life, Chemical and Earth Sciences. Theory and Practice*, eds. J.-C. G. Bünzli and G. R. Choppin, Elservier Science Publ. B.V., Amsterdam, 1989, Ch. 1, 1–41.
48 K. Binnemans, *Rare earth β-diketonate complexes: functionalities and applications*, Handbook on the Physics and Chemistry of Rare Earths, ed. K. A. Gschneidner Jr., J.-C. G.Bünzli and V. Pecharsky, Vol. 35, Ch. 225, Elsevier, Amsterdam, 2005.
49 P. A. Vigato and S. Tamburini, *Coord. Chem. Rev.*, 2004, **248**, 1717.
50 V. S. Sastri, J.-C. G. Bünzli, V. R. Rao, G. V. S. Rayudu and J. R. Perumareddi, *Modern Aspects of Rare Earths and Complexes*, Elsevier B.V., Amsterdam, 2003.
51 D. K. P. Ng, *Half-sandwich tetrapyrrole complexes of rare earths and actinides*, Handbook on the Physics and Chemistry of Rare Earths, eds. K. A. Gschneidner Jr., E. M. Eyring, and G. H. Lander, Vol. 32, Ch. 210, Elsevier Science B.V., Amsterdam, 2001.
52 R. M. Izatt, J. S. Bradshaw, S. A. Nielsen, J. D. Lamb and J. J. Christensen, *Chem. Rev.*, 1985, **85**, 271.
53 Z. Asfari, V. Böhmer, J. M. Harrowfield and J. Vicens, *Calixarenes 2001*, Kluwer Academic Publishers, Dordrecht, 2001.
54 J.-C. G. Bünzli, F. Besançon and F. Ihringer, in *Calixarenes for Separations*, eds. G. J. Lumetta, R. D. Rogers and A. Gopalan,

American Chemical Society, Washington D.C., 2000, Vol. 757, Ch. 14, 179–94.
55 D. M. Roundhill, *Prog. Inorg. Chem.*, 1995, **43**, 533.
56 I. Lukes, J. Kotek, P. Vojtisek and P. Hermann, *Coord. Chem. Rev.*, 2001, **216**, 287.
57 *The Chemistry of Contrast Agents in Medical Magnetic Resonance Imaging*, eds. Merbach, A. E. and Tóth, E., Wiley, London, 2001.
58 S. Liu, *Chem. Soc. Rev.*, 2004, **33**, 445.
59 D. Parker, *Coord. Chem. Rev.*, 2000, **205**, 109.
60 F. Renaud, C. Piguet, G. Bernardinelli, J.-C. G. Bünzli and G. Hopfgartner, *J. Am. Chem. Soc.*, 1999, **121**, 9326.
61 C. Piguet, C. Edder, S. Rigault, G. Bernardinelli, J.-C. G. Bünzli and G. Hopfgartner, *J. Chem. Soc., Dalton Trans.*, 2000, 3999.
62 J.-M. Lehn, *Supramolecular Chemistry. Concepts and Perspectives*, VCH, Weinheim, New York, Basel, Cambridge, Tokyo, 1995.
63 P. J. Stang and B. Olenyuk, *Acc. Chem. Res.*, 1997, **30**, 502.
64 J.-C. G. Bünzli and C. Piguet, *Chem. Rev.*, 2002, **102**, 1897.
65 C. Piguet, M. Borkovec, J. Hamacek and K. Zeckert, *Coord. Chem. Rev.*, 2005, **249**, 705.
66 S. Floquet, M. Borkovec, G. Bernardinelli, A. Pinto, L.-A. Leuthold, G. Hopfgartner, D. Imbert, J.-C. G. Bünzli and C. Piguet, *Chem. Eur. J.*, 2004, **10**, 1091.
67 M. A. Mortellaro and D. G. Nocera, *J. Am. Chem. Soc.*, 1996, **118**, 7414.
68 D. Parker and J. A. G. Williams, *Responsive luminescent lanthanide complexes*, Metal Ions in Biological Systems, eds. A. Sigel and H. Sigel, Vol. 40, Marcel Dekker Inc., New York, 2003.
69 T. Gunnlaugsson, J. P. Leonard, K. Senechal and A. J. Harte, *Chem. Commun.*, 2004, 782.
70 O. Reany, T. Gunnlaugsson and D. Parker, *J. Chem. Soc., Perkin Trans. 2*, 2000, 1819.
71 A. P. De Silva, H. Q. N. Gunaratne, T. E. Rice and S. Stewart, *Chem. Commun.*, 1997, 1891.
72 C. Li and W. T. Wong, *Chem. Commun.*, 2002, 2034.
73 T. Gunnlaugsson, J. P. Leonard, K. Senechal and A. J. Harte, *J. Am. Chem. Soc.*, 2003, **125**, 12062.
74 C. Bazzicalupi, A. Bencini, A. Bianchi, C. Giorgi, V. Fusi, A. Masotti, B. Valtancoli, A. Roque and F. Pina, *Chem. Commun.*, 2000, 561.
75 M. P. Lowe and D. Parker, *Chem. Commun.*, 2000, 707.
76 L. J. Charbonnière, R. Ziessel, M. Montalti, L. Prodi, N. Zaccheroni, C. Boehme and G. Wipff, *J. Am. Chem. Soc.*, 2002, **124**, 7779.
77 S. Petoud, S. M. Cohen, J.-C. G. Bünzli and K. N. Raymond, *J. Am. Chem. Soc.*, 2003, **125**, 13324.
78 Y. Y. Xu and I. Hemmilä, *Talanta*, 1992, **39**, 759.
79 G. Mathis, *Clin. Chem.*, 1995, **41**, 1391.
80 P. Hurskainen, *J. Alloys Comp.*, 1995, **225**, 489.
81 J. L. Yuan, G. L. Wang, H. Kimura and K. Matsumoto, *Anal. Biochem.*, 1997, **254**, 283.
82 E. R. Menzel, *Anal. Chem.*, 1989, **61**, 557A.
83 G. Vereb, E. Jares-Erijman, P. R. Selvin and T. M. Jovin, *Biophys. J.*, 1998, **74**, 2210.
84 D. J. Bornhop, D. S. Hubbard, M. P. Houlne, C. Adair, G. E. Kiefer, B. C. Pence and D. L. Morgan, *Anal. Chem.*, 1999, **71**, 2607.
85 D. J. Bornhop, J. M. M. Griffin, T. S. Goebel, M. R. Sudduth, B. Bell and M. Motamedi, *Appl. Spectrosc.*, 2003, **57**, 1216.
86 N. Weibel, L. J. Charbonnière, M. Guardigli, A. Roda and R. F. Ziessel, *J. Am. Chem. Soc.*, 2004, **26**, 4888.
87 A. Beeby, S. W. Botchway, I. M. Clarkson, S. Faulkner, A. W. Parker, D. Parker and J. A. G. Williams, *J. Photochem. Photobiol. B Biol.*, 2000, **57**, 83.
88 H. C. Manning, T. Goebel, R. C. Thompson, R. R. Price, H. Lee and D. J. Bornhop, *Bioconjugate Chem.*, 2004, **15**, 1488.
89 A. V. Chudinov, V. D. Rumyantseva, A. V. Lobanov, G. K. Chudinova, A. A. Stomakhin and A. F. Mironov, *Russ. J. Bioorg. Chem.*, 2004, **30**, 89.
90 S. Torelli, D. Imbert, M. Cantuel, G. Bernardinelli, S. Delahaye, A. Hauser, J.-C. G. Bünzli and C. Piguet, *Chem. Eur. J.*, 2005, **11**, 3238.
91 J. R. Lakowicz, G. Piszczek, B. P. Maliwal and I. Gryczynski, *ChemPhysChem*, 2001, **2**, 247.
92 G. Piszczek, B. P. Maliwal, I. Gryczynski, J. Dattelbaum and J. R. Lakowicz, *J. Fluoresc.*, 2002, **11**, 101.
93 H. J. M. A. Zijlmans, J. Bonnet, J. Burton, K. Kardos, T. Vail, R. S. Niedbala and H. J. Tanke, *Anal. Biochem.*, 1999, **267**, 30.
94 K. Binnemans and C. Görller-Walrand, *Chem. Rev.*, 2002, **102**, 2303.
95 B. Donnio, D. Guillon, D. W. Bruce and R. Deschenaux, in *Comprehensive Coordination Chemistry II: from Biology to Nanotechnology*, eds. J. A. McCleverty, T. J. Meyer, M. Fujita and A. Powell, Elsevier, Oxford, 2003, Ch. 7.9, 357–627.
96 L. J. Yu and M. M. Labes, *Appl. Phys. Lett.*, 1977, **31**, 719.
97 C. Piechocki, J. Simon, J. J. André, D. Guillon, P. Petit, A. Skoulios and P. Weber, *Chem. Phys. Lett.*, 1985, **122**, 124.
98 Y. G. Galyametdinov, G. I. Ivanova and I. V. Ovchinnikov, *Bull. Acad. Sci. USSR., D. Chem. Sci.*, 1991, **40**, 1109.
99 Y. G. Galyametdinov, G. I. Ivanova, A. V. Prosvirin and O. Kadkin, *Russ. Chem. Bull.*, 1994, **43**, 938.
100 K. Binnemans, Y. G. Galyametdinov, S. R. Collinson and D. W. Bruce, *J. Mater. Chem.*, 1998, **8**, 1551.
101 H. Deng, D. L. Gin and R. C. Smith, *J. Am. Chem. Soc.*, 1998, **120**, 3522.
102 H. Nozary, C. Piguet, P. Tissot, G. Bernardinelli, J.-C. G. Bünzli, R. Deschenaux and D. Guillon, *J. Am. Chem. Soc.*, 1998, **120**, 12274.
103 E. Guillet, D. Imbert, R. Scopelliti and J.-C. G. Bünzli, *Chem. Mater.*, 2004, **16**, 4063.
104 K. Driesen and K. Binnemans, *Liq. Cryst.*, 2004, **31**, 601.
105 K. Binnemans, Y. G. Galyametdinov, R. Van Deun, D. W. Bruce, S. R. Collinson, A. P. Polishchuk, I. Bikchantaev, W. Haase, A. V. Prosvirin, L. Tinchurina, I. Litvinov and A. Gubajdullin, et al., *J. Am. Chem. Soc.*, 2000, **122**, 4335.
106 Y. G. Galyametdinov, W. Haase, L. Malykhina, A. Prosvirin, I. Bikchantaev, A. Rakhmatullin and K. Binnemans, *Chem. Eur. J.*, 2001, **7**, 99.
107 S. Suárez, O. Mamula, D. Imbert, B. Donnio, D. Guillon, R. Scopelliti, C. Piguet and J.-C. G. Bünzli, *New J. Chem.*, 2005, **29**, 1323.
108 E. Terazzi, S. Torelli, J.-P. Rivera, J.-M. Benech, G. Bernardinelli, C. Bourgogne, B. Donnio, D. Guillon, D. Imbert, J.-C. G. Bünzli, A. Pinto, D. Jeannerat and C. Piguet, *J. Am. Chem. Soc.*, 2005, **127**, 888.
109 S. Suárez, D. Imbert, F. Gumy, C. Piguet and J.-C. G. Bünzli, *Chem. Mater.*, 2004, **16**, 3257.
110 S. Suárez, O. Mamula, D. Imbert, C. Piguet and J.-C. G. Bünzli, *Chem. Commun.*, 2003, 1226.
111 M. Kleinerman and S.-I. Choi, *J. Chem. Phys.*, 1968, **49**, 3901.
112 C. Görller-Walrand and K. Binnemans, *Spectral Intensities of f–f transitions*, Handbook on the Physics and Chemistry of Rare Earths, eds. K. A. Gschneidner, Jr. and L. Eyring, Vol. 25, Ch. 167, Elsevier Science B.V., Amsterdam, 1998.
113 K. Binnemans, L. Malykhina, V. S. Mironov, W. Haase, K. Driesen, R. Van Deun, L. Fluyt, C. Görller-Walrand and Y. G. Galyametdinov, *ChemPhysChem*, 2001, **2**, 680.
114 Y. G. Galyametdinov, L. Malykhina, W. Haase, K. Driesen and K. Binnemans, *Liq. Cryst.*, 2002, **29**, 1581.
115 J. Boyaval, C. Li, F. Hapiot, M. Warenghem, N. Isaert, Y. Guyot, G. Boulon and P. Carette, *Mol. Cryst. Liq. Cryst.*, 2001, **359**, 337.
116 K. Binnemans and D. Moors, *J. Mater. Chem.*, 2002, **12**, 3374.
117 R. Van Deun, D. Moors, B. De Fre and K. Binnemans, *J. Mater. Chem.*, 2003, **13**, 1520.
118 T. Welton, *Chem. Rev.*, 1999, **99**, 2071.
119 D. B. Williams, M. E. Stoll, B. L. Scott, D. A. Costa and W. J. Oldham, Jr., *Chem. Commun.*, 2005, 1438.
120 I. Billard, G. Moutiers, A. Labet, A. El Azzi, C. Gaillard, C. Mariet and K. Lützenkirchen, *Inorg. Chem.*, 2003, **42**, 1726.
121 P. Wasserscheid and T. Welton, *Ionic liquids in synthesis*, Wiley-VCH, Weinheim, 2005.
122 G. Moutiers and I. Billard, *Techniques de l'Ingénieur*, 2004 Report AF 6 712.
123 I. Billard, S. Mekki, C. Gaillard, P. Hesemann, G. Moutiers, C. Mariet, A. Labet and J.-C. G. Bünzli, *Eur. J. Inorg. Chem.*, 2004, 1190.
124 W. J. Gau and I. W. Sun, *J. Electrochem. Soc.*, 1996, **143**, 914.
125 A. Chaumont and G. Wipff, *Inorg. Chem.*, 2004, 5891.

126 A. E. Visser and R. D. Rogers, *J. Solid State Chem.*, 2003, **171**, 109.
127 M. P. Jensen, J. Neuefeind, J. V. Beitz, S. Skanthakumar and L. Soderholm, *J. Am. Chem. Soc.*, 2003, **125**, 15466.
128 K. Driesen, P. Nockemann and K. Binnemans, *Chem. Phys. Lett.*, 2004, **395**, 306.
129 S. Arenz, A. Babai, K. Binnemans, K. Driesen, R. Giernoth, A.-V. Mudring and P. Nockemann, *Chem. Phys. Lett.*, 2005, **402**, 75.
130 S. Kim, Y. T. Lim, E. G. Soltesz, A. M. De Grand, J. Lee, A. Nakayama, J. A. Parker, T. Mihaljevic, R. G. Laurence, D. M. Dor, L. H. Cohn, M. G. Bawendi and J. W. Frangioni, *Nature Biotechnol.*, 2004, **22**, 93.
131 R. Weissleder, *Nature Biotechnol.*, 2001, **19**, 316.
132 Y. Hasegawa, Y. Wada and S. Yanagida, *J. Photochem. Photobiol. C: Photochem. Rev.*, 2004, **5**, 183.
133 C. Strohhoefer and A. Polman, *Opt. Mater.*, 2003, **21**, 705.
134 D. Ananias, M. Kostova, F. A. Almeida Paz, A. Ferreira, L. D. Carlos, J. Klinowski and J. Rocha, *J. Am. Chem. Soc.*, 2004, **126**, 10410.
135 O. Guillou and C. Daiguebonne, in *Handbook on the Physics and Chemistry of Rare Earths*, eds. K. A. Gschneidner, Jr., J.-C. G. Bünzli and V. K. Pecharsky, Elsevier North Holland, Amsterdam, 2004, Vol. 34, Ch. 221.
136 T. S. Kang, B. S. Harrison, M. Bouguettaya, T. J. Foley, J. M. Boncella, K. S. Schanze and J. R. Reynolds, *Adv. Funct. Mat.*, 2003, **13**, 205.
137 Y. Hasegawa, K. Sogabe, Y. Wada and S. Yanagida, *J. Lumin.*, 2003, **101**, 235.
138 K. Driesen, R. Van Deun, C. Görller-Walrand and K. Binnemans, *Chem. Mater.*, 2004, **16**, 1531.
139 Yu. V. Korovin and N. V. Rusakova, *Rev. Inorg. Chem.*, 2001, **21**, 299.
140 B. S. Harrison, T. J. Foley, A. S. Knefely, J. K. Mwaura, G. B. Cunningham, T.-S. Kang, M. Bouguettaya, J. M. Boncella, J. R. Reynolds and K. S. Schanze, *Chem. Mater.*, 2004, **16**, 2938.
141 H. S. He, J. P. Guo, Z. X. Zhao, W. K. Wong, W. Y. Wong, W. K. Lo, K. F. Li, L. Luo and K. W. Cheah, *Eur. J. Inorg. Chem.*, 2004, 837.
142 H. S. Wang, G. D. Qian, M. Q. Wang, J. H. Zhang and Y. S. Luo, *J. Phys. Chem. B*, 2004, **108**, 8084.
143 G. A. Hebbink, L. Grave, L. A. Woldering, D. N. Reinhoudt and F. C. J. M. Van Veggel, *J. Phys. Chem. A*, 2003, **107**, 2483.
144 S. Faulkner, M.-C. Carrié, S. J. A. Pope, J. Squire, A. Beeby and P. G. Sammes, *Dalton Trans.*, 2004, 1405.
145 B. P. Burton-Pye, S. L. Heath and S. Faulkner, *Dalton Trans.*, 2005, 146.
146 R. Van Deun, P. Fias, P. Nockemann, A. Schepers, T. N. Parac-Vogt, K. Van Hecke, L. Van Meervelt and K. Binnemans, *Inorg. Chem.*, 2004, **43**, 8461.
147 F. Artizzu, P. Deplano, L. Marchio, M. L. Mercuri, L. Pilia, A. Serpe, F. Quochi, R. Orru, F. Cordella, F. Meinardi, R. Tubino, A. Mura and G. Bongiovanni, *Inorg. Chem.*, 2005, **44**, 840.
148 R. Van Deun, P. Fias, K. Driesen, K. Binnemans and C. Görller-Walrand, *PhysChemChemPhys*, 2003, **5**, 2754.
149 A. Casnati, F. Sansone, A. Sartori, L. Prodi, M. Montalti, N. Zaccheroni, F. Ugozzoli and R. Ungaro, *Eur. J. Org. Chem.*, 2003, 1475.
150 D. Imbert, S. Comby, A.-S. Chauvin and J.-C. G. Bünzli, *Chem. Commun.*, 2005, 1432.
151 S. Comby, D. Imbert, A.-S. Chauvin and J.-C. G. Bünzli, unpublished work, 2005.
152 D. Guo, C. Duan, F. Lu, Y. Hasegawa, Q. Meng and S. Yanagida, *Chem. Commun.*, 2004, 1486.
153 S. I. Klink, H. Keizer, H. W. Hofstraat and F. C. J. M. Van Veggel, *Synth. Met.*, 2002, **127**, 213.
154 Y. Shen, T. Riedener and K. L. Bray, *Phys. Rev. B.*, 2000, **61**, 11460.
155 D. R. Gamelin and H. U. Güdel, *Acc. Chem. Res.*, 2000, **33**, 235.
156 P. Gerner, O. S. Wenger, R. Valiente and H. U. Güdel, *Inorg. Chem.*, 2001, **40**, 4534.
157 S. Heer, K. Petermann and H. U. Güdel, *J. Lumin.*, 2003, **102–103**, 144.
158 C. Piguet and J.-C. G. Bünzli, *Chem. Soc. Rev.*, 1999, **28**, 347.
159 S. Faulkner and S. J. A. Pope, *J. Am. Chem. Soc.*, 2003, **125**, 10526.
160 M. Sakamoto, K. Manseki and H. Okawa, *Coord. Chem. Rev.*, 2001, **219–221**, 379.
161 K. Hanaoka, K. Kikuchi, H. Kojima, Y. Urano and T. Nagano, *Angew. Chem. Int. Ed.*, 2003, **42**, 2996.
162 R. Rodriguez-Cortinas, F. Avecilla, C. Platas-Iglesias, D. Imbert, J.-C. G. Bünzli, A. de Blas and T. Rodriguez-Blas, *Inorg. Chem.*, 2002, **41**, 5336.
163 C. Piguet, E. Rivara-Minten, G. Bernardinelli, J.-C. G. Bünzli and G. Hopfgartner, *J. Chem. Soc., Dalton Trans.*, 1997, 421.
164 C. Edder, C. Piguet, J.-C. G. Bünzl and G. Hopfgartner, *Chem. Eur. J.*, 2001, **7**, 3014.
165 M. Cantuel, G. Bernardinelli, D. Imbert, J.-C. G. Bünzli, G. Hopfgartner and C. Piguet, *J. Chem. Soc., Dalton Trans.*, 2002, 1929.
166 P. D. Beer, F. Szemes, P. Passaniti and M. Maestri, *Inorg. Chem.*, 2004, **43**, 3965.
167 P. Coppo, M. Duati, V. N. Kozhevnikov, J. W. Hofstraat and L. De Cola, *Angew. Chem. Int. Ed.*, 2005, **44**, 1806.
168 S. I. Klink, H. Keizer and F. C. J. M. van Veggel, *Angew. Chem. Int. Ed.*, 2000, **39**, 4319.
169 S. J. A. Pope, B. J. Coe, S. Faulkner, E. V. Bichenkova, X. Yu and K. T. Douglas, *J. Am. Chem. Soc.*, 2004, **126**, 9490.
170 N. M. Shavaleev, Z. R. Bell and M. D. Ward, *J. Chem. Soc., Dalton Trans.*, 2002, 3925.
171 S. J. A. Pope, B. J. Coe and S. Faulkner, *Chem. Commun.*, 2004, 1550.
172 N. M. Shavaleev, G. Accorsi, D. Virgili, Z. R. Bell, T. Lazarides, G. Calogero, N. Armaroli and M. D. Ward, *Inorg. Chem.*, 2005, **44**, 61.
173 P. B. Glover, P. R. Ashton, L. J. Childs, A. Rodger, M. Kercher, R. M. Williams, L. De Cola and Z. Pikramenou, *J. Am. Chem. Soc.*, 2003, **125**, 9918.
174 N. M. Shavaleev, L. P. Moorcraft, S. J. A. Pope, Z. R. Bell, S. Faulkner and M. D. Ward, *Chem. Eur. J.*, 2003, **9**, 5283.
175 N. M. Shavaleev, L. P. Moorcraft, S. J. A. Pope, Z. R. Bell, S. Faulkner and M. D. Ward, *Chem. Commun.*, 2003, 1134.
176 M. A. Subhan, H. Nakata, T. Suzuki, J.-H. Choi and S. Kaizaki, *J. Lumin.*, 2003, **101**, 307.
177 T. Sanada, T. Suzuki, T. Yoshida and S. Kaizaki, *Inorg. Chem.*, 1998, **37**, 4712.
178 S. F. Lincoln, *Helv. Chim. Acta*, 2005, **88**, 523.
179 N. André, T. B. Jensen, R. Scopelliti, D. Imbert, M. Elhabiri, G. Hopfgartner, C. Piguet and J.-C. G. Bünzli, *Inorg. Chem.*, 2004, **43**, 515.
180 S. J. A. Pope, A. M. Kenwright, S. L. Heath and S. Faulkner, *Chem. Commun.*, 2003, 1550.
181 S. J. A. Pope, A. M. Kenwright, V. A. Boote and S. Faulkner, *Dalton Trans.*, 2003, 3780.
182 M. A. Subhan, T. Suzuki and S. Kaizaki, *J. Chem. Soc., Dalton Trans.*, 2001, 492.
183 M. A. Subhan, T. Suzuki and S. Kaizaki, *J. Chem. Soc., Dalton Trans.*, 2002, 1416.
184 M. Cantuel, G. Bernardinelli, G. Muller, J. P. Riehl and C. Piguet, *Inorg. Chem.*, 2004, **43**, 1840.
185 F. S. Richardson, *Chem. Rev.*, 1982, **82**, 541.
186 J. P. Riehl and F. S. Richardson, *Chem. Rev.*, 1986, **86**, 1.
187 H. Tsukube and S. Shinoda, *Chem. Rev.*, 2002, **102**, 2389.
188 S. G. Telfer, N. Tajima, R. Kuroda, M. Cantuel and C. Piguet, *Inorg. Chem.*, 2004, **43**, 5302.
189 H. S. Tsukube, S. Shinoda and H. Tamiaki, *Coord. Chem. Rev.*, 2002, **226**, 227.
190 J. P. Riehl, in *'Encyclopedia of Spectroscopy and Spectrometry'*, ed. J. C. Lindon, G. E. Tranter, and J. L. Holmes, San Diego, 2000, p. 243 ff; J. P. Riehl and G. Muller, *Circularly polarized luminescence spectroscopy from lanthanides*, in *Handbook on the Physics and Chemistry of Rare Earths*, ed. K. A. Gschneidner Jr. and J.-C. G. Bünzli and V. Pecharsky, North Holland Publ. Co., Amsterdam, 1979, Vol. 34, Ch. 224, p. 289 ff.
191 S. C. J. Meskers and H. P. J. M. Dekkers, *J. Phys. Chem. A*, 2001, **105**, 4589.
192 D. Parker, *Chem. Soc. Rev.*, 2004, **33**, 156.

193 G. Muller, B. Schmidt, J. Jiricek, G. Hopfgartner, J. P. Riehl, J.-C. G. Bünzli and C. Piguet, *J. Chem. Soc., Dalton Trans.*, 2001, 2655.
194 G. Muller, J. P. Riehl, K. J. Schenk, G. Hopfgartner, C. Piguet and J.-C. G. Bünzli, *Eur. J. Inorg. Chem.*, 2002, 3101.
195 G. Muller, J.-C. G. Bünzli, J. P. Riehl, D. Suhr, A. von Zelewsky and H. Mürner, *Chem. Commun.*, 2002, 1522.
196 G. R. Motson, O. Mamula, J. C. Jeffery, J. A. McCleverty, M. D. Ward and A. von Zelewsky, *J. Chem. Soc., Dalton Trans.*, 2001, 1389.
197 T. Yamada, S. Shinoda, H. Sugimoto, J.-I. Uenishi and H. Tsukube, *Inorg. Chem.*, 2003, **42**, 7932.197.
198 R. S. Dickens, J. A. K. Howard, C. L. Maupin, J. M. Moloney, D. Parker, R. D. Peacock, J. P. Riehl and G. Siligardi, *New J. Chem.*, 1998, 891.
199 R. S. Dickins, S. Aime, A. S. Batsanov, A. Beeby, M. Botta, J. I. Bruce, J. A. K. Howard, C. S. Love, D. Parker, R. D. Peacock and H. Pushmann, *J. Am. Chem. Soc.*, 2002, **124**, 12697.
200 C. L. Maupin, D. Parker, J. A. G. Williams and J. P. Riehl, *J. Am. Chem. Soc.*, 1998, **120**, 10563.
201 G. Bobba, J. C. Frias and D. Parker, *Chem. Commun.*, 2002, 890.
202 J. C. Frias, G. Bobba, M. J. Cann, C. J. Hutchison and D. Parker, *Org. Biomol. Chem.*, 2003, **1**, 905.
203 R. A. Poole, G. Bobba, M. J. Cann, J. C. Frias, D. Parker and R. D. Peacock, *Org. Biomol. Chem.*, 2005, **3**, 1013.
204 A. Beeby, R. S. Dickins, S. FitzGerald, L. J. Govenlock, C. L. Maupin, D. Parker, J. P. Riehl, G. Siligardi and J. A. G. Williams, *Chem. Commun.*, 2000, 1183.
205 S. Aime, M. Botta, R. S. Dickins, C. L. Maupin, D. A. Parker, J. P. Riehl and J. A. G. Williams, *J. Chem. Soc., Dalton Trans.*, 1998, 881.
206 T. N. Parac-Vogt, K. Binnemans and C. Görller-Walrand, *J. Chem. Soc., Dalton Trans.*, 2002, 1602.
207 F. S. Richardson, D. H. Metcalf and D. P. Glover, *J. Phys. Chem.*, 1991, **95**, 6249 and references therein.
208 X. D. Hai, M. Q. Tan, G. Wang, Z. Q. Ye, J. Yuan and K. Matsumoto, *Anal. Sci.*, 2004, **20**, 245.
209 L. M. Fu, X. F. Wen, X. C. Ai, Y. Sun, Y. S. Wu, J. P. Zhang and Y. Wang, *Angew. Chem. Int. Ed.*, 2005, **44**, 747.
210 S. Floquet, M. Borkovec, G. Bernardinelli, A. Pinto, L.-A. Leuthold, G. Hopfgartner, D. Imbert, J.-C. G. Bünzli and C. Piguet, *Chem. Eur. J.*, 2004, **10**, 1091.